AR-010-247

DSTO-RR-0105

Structural Shape Optimisation by Iterative Finite Element Solution

R. Kaye and M. Heller

DSTO-RR-0105

DEPARTMENT OF DEFENCE

DEFENCE SCIENCE AND TECHNOLOGY ORGANISATION

Structural Shape Optimisation by Iterative Finite Element Solution

R. Kaye and M. Heller

Airframes and Engines Division
Aeronautical and Maritime Research Laboratory

DSTO-RR-0105

ABSTRACT

This report presents the development and automated numerical implementation of an iterative gradientless optimisation method for the analysis of problems relating to life extension of aircraft components. The method has been implemented to interface with the finite element code PAFEC, which does not normally have an optimisation capability. The key feature of the approach is to achieve constant boundary stresses, in regions of interest, by moving nodes on the stress concentrator boundary by an amount dependent on the sign and magnitude of the local hoop stress obtained from a previous iteration of a standard finite element analysis. The results of example problems are presented which include the optimisation of hole shapes in flat plates and the optimisation of the design of bonded reinforcements with a focus on minimising adhesive stress while maintaining the effectiveness of the reinforcement. In all cases significant stress reductions were achieved by way of the local shape changes. The method presented is considered a simple robust complementary method to the use of commercially available gradient based finite element optimisation software. It is also considered suitable for use with typical standard commercial finite element packages other than PAFEC.

RELEASE LIMITATION

Approved for public release

DEPARTMENT OF DEFENCE

DEFENCE SCIENCE AND TECHNOLOGY ORGANISATION

Published by

DSTO Aeronautical and Maritime Research Laboratory
PO Box 4331
Melbourne Victoria 3001

Telephone: (03) 9626 7000
Fax: (03) 9626 7999

AR-010-247
June 1997

APPROVED FOR PUBLIC RELEASE

Structural Shape Optimisation by Iterative Finite Element Solution

Executive Summary

Two common fatigue life extension practices which seek to favourably alter the local stress distribution near a stress concentrator in a RAAF aircraft component are: (i) modification of the existing local geometry by removing material, and (ii) addition of new material to the local region; such as the adhesive bonding of a composite patch. In both these cases an improved geometry (i.e. shape) is sought that minimises the magnitude of peak tensile stresses. However, the design of re-work shapes or bonded patches for RAAF aircraft components has typically been based on intuitive trial and error (or simplified analytical formulations). Subsequently the effectiveness of such design has usually been quantified using standard finite element analyses methods. It is believed that the use of optimisation procedures would significantly improve the effectiveness of such shape modification designs. However, finite element based optimisation procedures have not previously been used at AMRL in this context.

This report presents the development and automated numerical implementation of an iterative gradientless optimisation method for the analysis of problems relating to life extension of aircraft components. The method has been implemented to interface with the finite element code PAFEC, which does not normally have an optimisation capability. The key feature of the approach is to achieve constant boundary stresses, in regions of interest, by moving nodes on the stress concentrator boundary by an amount dependent on the sign and magnitude of the local hoop stress obtained from a previous iteration of a standard finite element analysis. The results of example problems are presented which include the optimisation of hole shapes in flat plates and the optimisation of the design of bonded reinforcements with a focus on minimising adhesive stress while maintaining the effectiveness of the reinforcement. In all cases significant stress reductions were achieved by way of the local shape changes. The method presented is considered a simple robust complementary method to the use of commercially available gradient based finite element optimisation software.

The procedure developed and implemented in this report has given AED the capability of determining optimal shapes for extending the fatigue life of critical regions in RAAF aircraft structural components.

Authors

R. Kaye

Airframes and Engines Division

Having completed a B. Eng at the University of New South Wales in 1981, Robert Kaye joined DSTO at AMRL in 1990 as a structural engineer with a background in full scale testing. Since that time he has mostly been occupied with the evaluation of air frame structural details and bonded repairs using finite element methods. This has included the analysis of repairs to fuselage skin lap-joints, wing skin planks and bulkhead frames. There has also been some involvement in the structural and mechanical development aspects of full scale static and fatigue test installations.

M. Heller

Airframes and Engines Division

Manfred Heller completed a B. Eng. (Hons.) in Aeronautical Engineering at the University of New South Wales in 1981. He was awarded a Department of Defence Postgraduate Cadetship in 1986, completing a PhD at Melbourne University in 1989.

He commenced work in Structures Division at the Aeronautical Research Laboratory in 1982. He has an extensive publication record focussing on the areas of stress analysis, fracture mechanics, fatigue life extension methodologies and experimental validation. Since 1992 he has lead tasks which develop and evaluate techniques for extending the fatigue life of ADF aircraft components and provide specialised structural mechanics support to the ADF. He is currently a Senior Research Scientist in the Airframes and Engines Division.

Contents

Notation

σ	stress in tangential (hoop) direction
Γ	contour of nodes on boundary
τ	shear stress in x, y co-ordinate system
v	Poisson's Ratio
d	movement of node in normal direction
E	elastic modulus
GPa	gigapascal
l	length of tapered region of patch
mm	millimetre
MPa	megapascal
i	node number
k	total number of nodes on boundary
m,n	local cartesion co-ordinates where n is normal to contour
r	characteristic length
s	step size scaling factor
t	patch thickness in tapered region as a function of x
x, y	global cartesian co-ordinates
Y	objective function to monitor convergence

Subscripts

i	node number
k	total number of nodes on boundary
o	refers to initial patch thickness
th	threshold value
av	average value

Superscripts

a	value after smoothing
max	maximum value

List of Abbreviations

AMRL	Aeronautical and Maritime Research Laboratory
FORTRAN	computer language for FORmula TRANslation
FFVH	fuel flow vent hole
FFVH13	fuel flow vent hole number 13
MSC/NASTRAN	commercial structural analysis program
PAFEC	Program for Automated Finite Element Calculations
PAFBLOCK	Feature in PAFEC for generating a group of elements
RAAF	Royal Australian Air Force

1. Introduction

AMRL has a continuing focus on implementing and developing methods suitable for the fatigue life extension of RAAF aircraft structural components. These methods are either directed at delaying the onset of crack initiation, and/or reducing the rate of crack growth at critical stress concentrating locations. These critical locations are often on free boundaries of structural components, and have a local geometry such that they are subjected to elevated cyclic tensile stresses when the airframe undergoes service loading. Two common life extension practices which seek to alter, in a favourable manner, the local stress distribution near a stress concentrator are: (i) modification of the existing local geometry by removing material, and (ii) addition of new material to the local region; for example by using an adhesively bonded reinforcement or an interference fitted component. In both these cases an improved geometry (i.e. shape) that minimises the peak magnitude of tensile stresses at a stress concentrating local region is desirable.

Finite element analysis provides a powerful tool for determining the stresses for a given geometry, and potentially for determining an optimised geometry to minimise the stress concentration. However, while finite element analyses have been extensively used at AMRL, it is important to note that finite element based optimisation procedures have not previously been applied at AMRL. In the past, rework shapes have typically been developed by using intuitive trial and error, and then their effectiveness quantified using standard finite element analyses. Similarly, in the case of bonded repairs, the initial design has typically been based on simplified analytical formulations, and then finalised by undertaking standard finite element analyses. Often the design of the bonded repairs has been confined to rectangular patches of constant thickness with linear tapering at the ends.

A number of finite element based approaches have been given in the literature for shape optimisation to minimise stress concentrations. In all these approaches the initial geometry is modified between iterations of a number of finite element analyses, until convergence of the peak stress to a suitable value has been achieved. A number of procedures can be employed for iterating the shape, and these include sensitivity analysis methods [1-5], gradientless methods [6-10] and layout methods [11-13].

In this paper we develop a simple, efficient gradientless computational method that can be used with any standard commercial finite element package for minimising stress concentrations. The driving force for the method is to achieve constant boundary stresses by correctly moving boundary nodal positions, in this sense it has most in common with the work of Schnack [6,7] and Mattheck *et al.* [8-10]. However, there are significant differences, primarily in the algorithm for determining new nodal position between iterations. In Section 2, a brief discussion of various finite element based shape optimisation approaches, including sensitivity, gradientless and layout methods, are given. In Section 3 a moving boundary method is postulated and presented for gradientless shape optimisation, using only the results of standard finite

element methods, in an iterative manner. In this approach nodes on the stress concentrator boundary are moved by an amount dependent on the sign and magnitude of the local hoop stress, obtained from a previous iteration of a standard finite element analysis. The results obtained from application of the method to sample problems involving stress concentrators in two dimensional plates are presented in Section 4. Subsequently in Section 5, numerical examples relating to bonded repairs in two dimensions are given. In the appendix software for the automated implementation of the procedure is presented for use with the PAFEC finite element package.

2. Comments on Finite Element Based Shape Optimisation Methods

2.1 Sensitivity analysis methods

Approaches based on sensitivity analysis require stress gradient information to be determined, so that the sensitivity of the objective function to boundary movements (i.e. shape change) at the stress concentrator can be quantified [1-5]. Most industry-standard finite element analysis software codes which have an optimisation capability use this approach. However, many commercial finite element codes have no optimisation capability. While sensitivity analysis is a powerful general method for optimisation, it can also be relatively demanding on computer time. Also significant is the fact that typically a great deal of effort is required (compared to standard finite element analyses) to generate a suitable initial model specification to obtain a successful result, with mesh distortion and appropriate specification of the objective function being particular problems. In the open literature a number of papers deal with the development of this method and apply it to relatively simple geometries. A particular focus has been on developing methods to reduce computational time. Surprisingly, to date very few examples are available in the literature discussing applications to more complex geometries.

2.2 Gradientless analysis methods

In gradientless analysis approaches stress derivatives are not used to determine optimal geometries, hence they are typically much simpler to implement, or use with standard (i.e. non-optimisation) finite element codes. The driving force for these methods is to determine a boundary shape, such that there is a constant or near constant stress distribution around the boundary. Previous work [6-10,14] has shown that such a situation results in a minimised peak stress around the boundary, except for the presence of structural details that restrict shape changes. Schnack *et al* [6,7] and Mattheck *et al.* [8-10] in particular have used finite element based methods to determinal optimal shape changes. However, the logic that these two authors respectively use to determine the new shape is completely different.

The work of Mattheck *et al.* is based on the interesting observations of shape optimisation in living organisms such as in trees and animal bones. As part of the evolutionary process many such 'living structures' appear to have been able to add material in regions of high stress and reduce material in regions of low stress to bring about an optimal shape that produces a constant Von Mises stress distribution on the free surface. To mimic this process for engineering structures, he uses an iterative approach as follows. First, undertake a standard finite element run to determine stresses on the boundary. Second, do a subsequent analysis in which an adhesive layer is added to the boundary, and is allowed to swell or contract in proportion due to the previously determined boundary stresses (which have been converted to an equivalent temperature distribution). The amount of swelling or contraction of the adhesive layer determines where to add material or remove material in the next finite element analysis, which is where the next iteration occurs.

In the work of Schnack *et al*, an extension to the fade away hypothesis of Neuber, for minimising peak notch stresses is used. There are three key ideas in Schnack's work. Firstly, that a change in the curvature at a point on a notch surface has a significant effect on the magnitude of the tangential stress at that point. Secondly, the higher the peak stress at a point on the notch, the more the stresses will fade away as the distance from the high stress zone increases. Thirdly, the magnitude of the maximum stress can be reduced by increasing the minimum stress on the notch surface. Schnack's finite element implementation starts by completing a standard analysis and determining tangential stresses at location around the hole boundary. Then the boundary nodes near the location of maximum tangential stress are moved to increase the local radius of curvature at that point. Similarly the nodes near the location of minimum tangential stress are also moved to decrease the local curvature. At the same time all other nodes around the boundary are moved to achieve a smooth transition of curvature between these two extreme points. With these new nodal positions, another finite element analysis is then undertaken and the process repeated until convergence is achieved.

2.3 Layout analysis methods

In typical layout optimisation [11-13], a highly discretised finite element mesh is used, of uniform element size, for a given design space. Then, subject to fixed geometry constraints, lightly stressed elements from a finite element model are removed or as a minor variation, the stiffness of lightly stressed elements is successively reduced. This approach then leads to the generation of many voids, so that in the limit open frame, truss-like structures can be created which are approximately uniformly stressed. However, if desired, the generation of multiple holes can be suppressed [13], so that only the geometry of one hole is modified (i.e. by removing only elements only that are at the hole boundary). Typically, although the general hole shape will be correct, the boundary will 'jagged'. Therefore another finite element analysis is then needed (using a fitted smooth boundary) to determine the appropriate stress concentrations. Hence these methods, although generally not able to generate smooth boundaries, appear

effective in determining an approximate shape, which can be used if desired as a starting geometry for analysis by other methods.

3. Moving Boundary Method

3.1 General description

Here we aim to develop a simple, efficient gradientless computational method that can be used with any standard commercial finite element package for minimising stress concentrations. The driving force for the method is to achieve constant boundary stress by correctly moving boundary nodal positions, in this sense the present method has most in common with the works of Schnack [6,7] and Mattheck *et al* [8-10] and their co-workers. However, there are significant differences in the present approach, primarily in the algorithm for determining new nodal positions between iterations, as detailed in the following sections.

Consider Figure 1 which shows a hole (stress concentrator) with boundary, Γ on which there are a number of nodes $i = 1, k$, under an arbitrary remote loading. The tangential stress will vary around the boundary due to remote loading as shown schematically in Figure 2. Let us use the logic of Mattheck (and others) and add material where stresses are high and remove it where stresses are low. The question is then what should the relative amounts of material to be added or removed be. A simple postulate would be to require the amount of material added or removed at any point on the boundary to be directly proportional to the difference between the local tangential stress and a suitable reference value, and this process can then be repeated iteratively until a reduced stress concentration has been achieved. Hence the amount to move a given node i on the boundary (in the normal direction) can be written as,

$$d_i = \left(\frac{\sigma_i - \sigma_{th}}{\sigma_{th}}\right) rs \qquad (1)$$

where positive d_i indicates material addition, σ_i is the tangential stress at node i on the boundary, σ_{th} is a threshold boundary hoop stress, r is an arbitrary characteristic length such as initial hole radius, and s is an arbitrary step size scaling factor typically in the range of 0.1–0.4.

A number of interesting features immediately become apparent, particularly in relation to the selection of the parameter σ_{th}, as follows: (i) if we select σ_{th} less than the maximum, but more than the minimum stress determined from the previous iteration, material will be both added and removed at various locations around the boundary, (ii) if we select σ_{th} the same or greater than the maximum stress determined from the previous iteration, the boundary will be moved to remove material only, and (iii) if we select σ_{th} to be the same or less than the minimum stress

determined from the previous iteration, the boundary will be moved to add material only. If we are reworking a stress concentrator in an existing component, we must use option (ii) or option (i) with a further constraint on boundary movements so that material is not added (i.e. $d_i < 0$).

This method is suitable for implementation with a standard finite element code that allows for movement of nodes after the completion of an analysis. The procedure is shown in the simple flow chart given in Figure 3. For such an iterative procedure an appropriate objective function, Y, to monitor solution convergence can be written as

$$Y = \frac{\sqrt{\sum_{i=1}^{i=k} (\sigma_i - \sigma_{th})^2}}{k-1} \qquad (2)$$

Clearly, as Y approaches zero, the stresses become more uniform around the boundary. It should be noted that a completely uniform distribution of stresses around the boundary can only be achieved for a restricted set of problems. The approach was implemented with the finite element code PAFEC, and this is described in the Appendix A. It should be noted that in the implementation with PAFEC, only the nodal movements at the stress concentrator boundary need to be specified. Internal nodes are automatically moved in a proportionate manner by making use of an element generation feature named PAFBLOCKs. PAFBLOCKs are typically four sided subregions in the finite element model consisting of a number of elements. Only the location of corner nodes and the number of elements along the PAFBLOCK sides need to be specified, in order for proportionately sized internal elements to be created. Typically for the analysis of the example problems described in Section 4, there were two elements per PAFBLOCK along the moving boundary.

3.2 Smoothing of nodal movements

In the course of preliminary analyses it was found that localised effects in some cases disrupted the solution process, particularly for highly refined meshes. In these cases boundary node stresses were found to be highly sensitive to the positions of neighbouring boundary nodes. For example, a node protruding slightly from the boundary had a very low stress and was hence moved too far outwards (away from the hole centre) at the next iteration. The neighbouring nodes would then be left protruding and be moved even further in the next iteration. The result of this is that alternate nodes would 'leap-frog' each other by increasing amounts, eventually causing fatal mesh distortion. To circumvent this potential problem for all analyses, nodal positions as defined by displacements given in Equation 1, were adjusted using three point averaging to include the effect of the two neighbouring nodal positions as follows:

$$x_i^a = (x_{i-1} + x_i + x_{i+1})/3 \qquad (3)$$

$$y_i^a = (y_{i-1} + y_i + y_{i+1})/3 \qquad (4)$$

where x , y refer to the nodal co-ordinate positions determined using displacements given by Equation (1), and x^a, y^a refer to the values after smoothing.

4. Numerical Examples Relating to Holes in Plates

In this section the results obtained from application of the method to sample problems involving stress concentrators in two dimensional plates are presented. For all analyses a linear elastic constitutive model was used with Young's modulus E = 70 000 MPa, and Poisson's ratio v = 0.32. For all cases rework optimisation analyses were undertaken where only material removal occurs. Hence all nodal movements were constrained such that $d_i < 0$. Also, in each case unless otherwise noted, the threshold value of stress used in Equation (1) was defined as $\sigma_{th} = \sigma_{av}$, where

$$\sigma_{av} = \frac{\sum_{i=1}^{i=k} \sigma_i}{k} \qquad (5)$$

For all cases involving automated boundary nodal movement, three point smoothing was used as described in section 3.2.

4.1 A square hole in a 2:1 biaxial stress field

For this analysis the plate geometry as shown in Figure 4 was considered. Here the large square plate contains a square centrally located hole with 20 mm long sides. A remote 2:1 biaxial stress field is applied to the plate, where the applied stresses are 50 MPa along the edges x=±100 mm and 100 MPa along the edges y=±100 mm. Hence one feature of this initial geometry (with the sharp corner) is that significant changes in the shape are expected, and therefore is considered a good test problem.

Due to symmetry, only one quarter of the plate was modelled in the finite element analysis, and the initial mesh discretisation using 4 noded elements is shown in Figure 5. The optimisation procedure detailed in Section 3 was used with the parameters r = 10 mm, and s = 0.3. The solution geometry obtained after 25 iterations is shown in Figure 6. It can be seen that the boundary is positioned entirely outside the initial square opening as required. As expected, the final shape is the known solution of an

ellipse with an aspect ratio of two to one for the major and minor axes [14]. For this solution the tangential stresses along the boundary were essentially constant with a range of 152.2 to 159.2 MPa, noting that the peak stress for the initial geometry was 535 MPa at the location x=y=10 mm. The contours given in Figure 6 show the distribution of maximum absolute principal stress, which on the hole boundary is equivalent to the tangential stress.

To determine the influence of the value of the step factor s, the analyses were repeated taking different values of this parameter. The relevant results are given in Figure 7 where the objective function versus iteration number is plotted for four different step factors. It can be seen that a step factor of 0.4 causes the solution to fail after 4 iterations when the boundary over shoots the solution. The correct shape is obtained for step factors smaller than this with obviously more iterations required as the step factor is reduced. At a step factor of 0.35 a successful solution is achieved but failure almost occurs at iteration 5. Robust successful solutions are obtained at values of 0.3 and 0.2, where it is seen that the objective function decreases monotonically with iteration number.

4.2 A round hole in a 4:1 biaxial stress field

For this analysis the plate geometry as shown in Figure 8 was considered. Here the large rectangular plate contains a circular centrally located hole of 20 mm diameter. A remote 4 : 1 biaxial stress field is applied to the plate, where the applied stresses are 50 MPa along the edges x=±100 mm and 200 MPa along the edges y=±100 mm. One feature of the initial geometry is that there is a region of compressive boundary stress, unlike the previous example.

Due to symmetry, only one quarter of the plate was modelled in the finite element analysis, and the initial mesh discretisation is shown in Figure 9. To improve accuracy a highly refined mesh consisting of 8 noded isoparametric quadrilaterals was used. The optimisation procedure detailed in Section 3 was applied with the parameters r = 10 mm and s =0.1. The solution geometry obtained after 250 iterations is shown in Figure 10. As expected the final shape is very close to the known solution of an ellipse with an aspect ratio of four to one for the major and minor axes [14], which is positioned entirely outside the circular opening as required. The tangential stress distribution around the hole boundary is shown in Figure 11. For this solution the tangential stresses along the boundary were essentially constant (except for one nodal position) with a stress range of 250 to 275 MPa, noting that the peak stress for the initial geometry was 550 MPa at the location x=10 mm and y=0 mm. For the selected step factor, it can be seen that the optimisation process was relatively slow to converge (particularly after the 50th iteration) as shown in Figure 12. One reason for this is believed to be due to the fact that the sensitivity between the length of the ellipse and the boundary stress is very low. Along the sides of the ellipse, very small nodal movements are required to find the optimal solution and there is a high level of dependence between the nodes. For the last 100 iterations it was necessary to turn off

the three point smoothing as it was prone to stifle the very small nodal movements. From the monotonically reducing objective function shown in Figure 12, it is clear that use of a larger step factor would have reduced the number of iterations required. The compressive stress region in the initial configuration did not effect the performance.

4.3 Corrosion removal in a uniaxial stress field

The size of full depth skin corrosion removal in aircraft structures is often restricted by neighbouring structural details. In the present analysis the optimisation procedure is applied to a problem which addresses this issue. For this analysis the plate geometry as shown in Figure 13 was considered. Here the large rectangular plate contains a centrally located circular hole of 12 mm diameter. A remote uniaxial stress field of 100 MPa is applied to the plate along the edges y=±100 mm. The key feature is that allowable material removal is constrained by the lines at y=±12 mm.

Due to symmetry, only one quarter of the plate was modelled in the finite element analysis, and the initial mesh discretisation is shown in Figure 14. Separate analyses were conducted using either all four noded or all eight noded elements. A manual implementation of the moving boundary method described in Section 3 was used. The optimisation was performed by manually moving PAFBLOCK corner nodes based on a chosen threshold stress and the values of boundary tangential stress. Where boundary hoop stress was below the threshold value, nodes were moved inwards to the threshold stress contour of maximum principle stress. The new coordinates were edited into the PAFEC data file of the previous iteration The solution geometry obtained after 14 iterations is shown in Figure 15. It can be seen that a uniform tangential stress occurs over the curved region of the boundary, which is also shown more clearly in Figure 16. The peak stress on the hole boundary was initially 311 MPa which has been reduced to essentially a constant value along the curved part of the boundary, in the range 167 to 178 MPa. There is good agreement between the analyses using either all 4 noded or all 8 noded elements, although as expected the 8 noded solution is better (i.e. less deviation from the mean along the curved boundary).

This example highlights the disadvantages of using Von Mises stress as a criterion for removing material, as used by some authors. Because of its root-mean-square formulation, boundary regions with compressive tangential stresses will have positive Von Mises values. Hence for such situations the adoption of the Von Mises based removal criteria would erroneously **not remove** material in these regions.

At the level of mesh refinement used, the abrupt corner shown in Figure 15 is free of raised stresses because of the unidirectional remote loading and the optimal rework shape. Any transverse load component would have led to a rounded shape in this corner region. It is interesting to note that the curved part of the boundary is neither elliptical or circular in form and is unlikely to be obtained by analytical methods.

4.4 Inclined oval hole in a uniaxial stress field (representative of F-111 fuel flow vent hole number 13)

As discussed in the previous example the shape of a rework is often constrained by geometric limits. This issue is further explored in the present example. For this analysis the plate geometry as shown in Figure 17 was considered. Here the large rectangular plate contains a centrally located oval shaped hole inclined at 16 degrees to the direction of uniaxial loading. The remote uniaxial stress field of 100 MPa is applied to the plate along the edges y=±140 mm. The key feature of the analysis is that material removal is constrained by the line shown in Figure 17, which represents a severe geometric constraint. This geometry has been chosen to be approximately representative of the fuel flow vent hole number 13 (FFVH13) region in the stiffener near the upper wing skin of the F-111 wing pivot fitting (which is a well known crack initiation site [15]). The plate geometry shown in Figure 17 is a two dimensional idealisation representing the stiffener, while the location of the constraint line corresponds to the location of the upper wing skin, with its thickness in the out of plane direction. In recent years the FFVH13 region has been subjected to grind-out rework profiles to remove service cracks and reduce the extent of the stress concentration to some extent [15].

The initial mesh discretisation for this problem, consisting of four noded elements, is shown in Figure 18. The optimisation procedure detailed in Section 3 was applied with the following parameters: (i) $\sigma_{th} = 0.5(\sigma_{av} + \sigma_i^{max})$, (ii) r = 6.35 mm, and (iii) s = 0.3. Iterations were continued until the reduction in tangential stress at point A became less than 1%. The geometry at the final iteration is shown in Figure 19, while the associated distribution of tangential stress around the hole boundary is shown in Figure 20. It can be seen that the process provided a good result in the critical region of point A. Here the initial peak stress of 309 MPa was reduced to a value of 171 MPa which was rendered uniform in the local region (i.e. nodes 11 to 27). However near point B (nodes 37 and 42) it can be seen that the presence of the constraint line has reduced the benefit of the optimisation process. Away from the constraint line the final shape is approximately elliptical in form. This example has demonstrated clearly that shape optimisation results are highly dependent on the direction of the surrounding principle stresses, in conjunction with the location of geometric constraints. It has also shown that near point B the initial geometry was close to optimal.

5. Numerical Examples Relating to Bonded Reinforcements

Bonded reinforcements and repairs to engineering components function primarily by transferring load from the component to the patch by shear deformation of the adhesive. This reduces the magnitude of strains in the repaired component and typically results in increased fatigue lives and static strength. One issue concerning the

improved design of bonded repairs which needs to addressed is the existence of large peaks in the adhesive shear strain distribution. For example, a severe peak typically occurs near the *end of the patch*. Such peaks have the potential to cause failure of the adhesive system and compromise the performance of the repair. In this section the method explained in section 3 is slightly modified to extend its application to the optimisation of the shape of the bonded reinforcement, while minimising the adhesive stress levels. Two example problems were considered, where in each case a two dimensional analysis was undertaken using a linear elastic constitutive model. In the first case the patch thickness was varied continuously while in the second, for a given patch design, the adhesive thickness was varied continuously.

5.1 Bonded joint taper

The configuration under study was a double lap joint as shown in Figure 21. It should be noted that this geometry is representative of a two dimensional idealisation of a bonded repair to a cracked plate. The inner adherend is a plate of 4 mm thickness which is loaded by a remote stress of 100 MPa. An outer adherend (i.e. patch) is bonded to each side of this plate by an adhesive layer having a uniform thickness of 0.15 mm. Thereby, symmetry is retained with respect to the plate mid-plane (y=0), and hence plate bending is eliminated. The thickness of each patch is denoted t_o and is 2 mm. As is commonly advocated, an initial linear taper with a 1:10 slope was used at the ends of each patch to reduce the magnitude of the adhesive stress concentration at the end of the patch. For this analysis a linear elastic constitutive model was used to model the plate and the patch with Young's modulus E = 70 000 MPa, and Poisson's ratio v = 0.32 In this optimisation we wish to change the shape of the tapered region to achieve a constant adhesive stress distribution. The procedure used was to reduce the patch thickness (at a given x co-ordinate) where the adhesive stresses were high, while increasing patch thickness where adhesive stresses were low. Hence a slight variation of Equation (1) to represent movement of nodes on the free boundary of the patch was used as follows

$$d_i = -(\frac{\tau_i - \tau_{th}}{\tau_{th}})rs \qquad (6)$$

where positive d_i indicates material addition from the patch outer boundary, τ_i is the shear stress at the adhesive midplane node i, τ_{th} is a threshold shear stress at the adhesive midplane, and r and s are as previously defined.

Due to symmetry, only one quarter of the joint was modelled in the finite element analysis, and the initial mesh discretisation is shown in Figure 22(a). The mesh consisted of 4 noded quadrilateral elements. A very dense mesh was used near the end of the patch to accurately model the high stress gradients in this region. For the adhesive a Young's Modulus of 840 MPa and a Poisson's Ratio of 0.3 was used. Other

material properties were as per section 5.1. The optimisation procedure was applied with the parameters r = 2 mm and s =0.1. One further practical constraint was introduced such that the patch thickness could not be less that 0.01 mm and not greater than 2 mm. The solution geometry obtained after 89 iterations is shown in Figure 22(b). As a comparison a one dimensional theoretical analysis given in [16] was found to give the profile shown in Figure 22(c). The equation from [16] defining the thickness in the tapered region as a function of position is

$$t = \frac{t_o x}{2l - x} \qquad (7)$$

where x is the distance from the start of the tapered region, t_o is the maximum thickness of the patch, and l is the length of the tapered region.

In Figure 23 the adhesive shear stresses are plotted for the following three taper profiles: (i) linear taper, (ii) numerically optimised taper, and (iii) analytically optimised taper [16]. It can be seen that the process provided a good result in reducing the peak shear stress, and rendering the shear stresses relatively uniform. Here the initial peak stress of 8.2 MPa for the linear taper case has been reduced by 30%. The one dimensional analysis gives a similarly significant reduction in peak adhesive stress. It is included here as a convenient comparison for this particular loading case. It must be noted that the advantage of the finite element method is that key parameters such as loading type and material properties are easily changed, and their modification is expected to pose no particular difficulty.

It is interesting to note that for the given inner adherend, a reduction in the adhesive peak at the end the patch can only be achieved through changing one or more of the material or geometric properties of the adhesive or the patch, near the end of the patch [17]. For example by increasing the adhesive thickness. While the optimisation process has been demonstrated for the case of minimising adhesive shear stress, it is believed other stress quantities, such as von Mises stress could have been selected.

5.2 Bonded repair to F/A-18 470 bulkhead

For this problem a semi-symmetric two dimensional MSC/NASTRAN finite element model obtained from reference [18] was used as a starting point. The relevent finite element geometry and mesh is shown in Figure 24. The location at Point A is a known crack initiation site for the bulkhead under the action of flight loads, due to the stress magnification in this local region. One life extension option under consideration at AMRL for reducing the magnitude of the stress concentration involves bonding an 8 ply boron patch to the critical region of the bulkhead. For convenience a PAFEC finite element model was developed to represent the substructured critical local region as shown in Figure 25. Here it can be seen that extra material was added to the right of the substructured region to enable correct distribution of local stresses. Hence the

magnitudes of the two uniaxial loads (342386 N and 42675 N) were chosen such that the stresses along the line of symmetry were the same as those given in the full MSC/NASTRAN model.

The finite element mesh for the substructured region with the 8 ply boron/epoxy patch is shown in Figure 26. For this analysis the boron patch was treated as an isotropic material with a Young's Modulus of 213,000 MPa and a Poisson's Ratio of 0.3. The material properties of the plate and adhesive were as used in Section 5.1. Here the adhesive thickness was constant at 0.13 mm and the patch thickness was 1.04 mm. The Von Mises stress results for the adhesive are given in Figure 29, with the associated reduction in stresses at point A in the bulkhead being 34% as compared to the unpatched results. From Figure 29 it can be seen that the adhesive Von Mises stresses vary along the joint and peak at point B. Clearly, an improved repair design would require a more uniform adhesive stress distribution, with an associated reduced peak value.

To optimise the adhesive stress distribution, the same procedure as given in Section 5.1 was used, except in this case the thickness of the adhesive layer was varied. This was achieved by moving nodes on the interface between the adhesive and the patch using the relation given in equation (6) with slight modification. Here the shear stress terms are replaced by Von Mises stress, and the adhesive thickness is increased at high stress regions and reduced at low stress regions. For this analysis the location of the outer boundary of the patch remains fixed for all iterations. The initial geometry of the adhesive layer consisted of a uniform thickness of 0.13 mm. While for the patch, the initial geometry was selected to have the following outer profile (i) nodes 1 to 5 were on the arc of a circle of radius 25 mm, and nodes 5 to 12 were on a straight line. Hence the patch had a variation in cross sectional thickness in the y direction, with the thicknesses at nodes 1, 3, 5 and 12 being 3.12, 2.92, 2.67 and 1.39 mm respectively. The optimisation procedure was applied with the parameters r = 1.5 mm and s =0.1. One further practical constraint was introduced such that the adhesive thickness could not be less than 0.13 mm.

The bonded repair geometry shown in Figure 27 was achieved after 47 iterations. This profile has a much greater stress reduction at point A (42%) and a more uniform adhesive stress distribution with a lower peak value, as compared to the standard patch design. To enable a better comparison with the nominal 8 layer patch case the iteration process was continued until the same stress reduction of 34% (after a further 53 iterations) was achieved at point A (in this process the adhesive layer becomes thicker). The final bonded repair geometry shown for this optimisation analysis is shown in Figure 28, and the adhesive stresses are given in Figure 29. It can be seen that the adhesive stresses have been further reduced and remain uniform. As can be expected, these results are consistent with the trend that generally in bonded reinforcement analyses, a lower patch effectiveness is associated with a lower adhesive stress.

6. Discussion

6.1 Typical results

The example problems that have been presented (along with those in the prominent literature) show that there are often large benefits to determining the optimal shape for a given structural detail under specified loading conditions. Reductions in peak stress of 30% and upwards can be achieved by accurate shaping of the boundary. The use of circular form shapes in fatigue prone structures is a poor alternative to the optimal free form shape in cases where the principal stress directions are known not to vary with load case. For many problems the optimal solution is characterised by uniform boundary stresses in the critical region, as discussed in Section 2.2 and demonstrated by the results presented in Sections 4 and 5.

In relation to optimisation of bonded repairs the problem of optimal shaping away from a cracked region is solved. Examples are presented with good results showing two distinct options. In the first option the patch thickness is varied continuously to provide a reduced and uniform adhesive stress distribution while still maintaining the same load transfer to the patch. In the second, for a given patch design, the adhesive thickness is varied continuously to give a reduced and uniform adhesive stress distribution while still effectively reducing stress in the reinforced component.

6.2 Numerical implementation issues

It is believed that the method developed here is a simple approach that can be adapted to suit finite element systems that do not provide an optimisation feature. For example the software developed to interface with the PAFEC finite element code (Appendix A) contains only several hundred lines of code with minimal branching.

In some of the example problems highly refined meshes were used which clearly increased the number of iterations required. This was not considered a concern since the total solution time was fast. However if solution time is a concern, one obvious tactic is not to overly refine the mesh. Furthermore, consideration can also be given to using a coarse mesh initially and then changing to a more refined version when the optimal solution is obtained. Similarly no concerted attempt was made to minimise the number of iterations by changing the parameters in Equation (1), again because of the fast solution time. Nevertheless if desired, it is believed that there is significant scope to change these key parameters without degrading the accuracy of the solution. Similarly while a simple three point smoothing method was successfully applied to determine nodal displacements, a more sophisticated smoothing method could readily be used if desired.

The appropriate choice of the threshold stress in Equation (1) is considered a powerful feature allowing either material removal or addition, or a weighted combination of

both. It is also interesting to note that because of the formulation of Equation (1), the absolute magnitude of boundary movement steps decreases automatically with increasing iteration number, as the optimal solution is approached. Hence the use of a uniform step factor was found to be very effective.

7. Conclusion

This report presents the development and automated numerical implementation of a gradientless optimisation method for the analysis of problems relating to life extension of aircraft components, namely (i) shape reworking of stress concentrators and (ii) shape changes for bonded reinforcements. The method has been implemented to be used in conjunction with the finite element code PAFEC, and it is considered suitable for use with other typical standard commercial finite element packages. The key feature of the approach is to achieve constant boundary stresses in regions of interest, by correctly moving boundary nodal positions. Typically nodes on the stress concentrator boundary are moved by an amount dependent on the sign and magnitude of the local hoop stress (relative to a selected threshold value) obtained from a previous iteration of a standard finite element analysis. The results of the numerical examples presented demonstrate the effectiveness of the approach that has been developed.

For the example rework problems that have been presented, along with those in the prominent literature, it has been shown that there are often large benefits brought about by finding the optimal shape for a given structural detail. Reductions in peak stress of 30% and upwards can be achieved by accurate shaping of the boundary geometry. The use of circular or even elliptical form shapes in fatigue prone structures is a poor alternative to the optimal free form shape. In relation to optimisation of bonded repairs the problem of optimal shaping away from a cracked region has been solved. Examples are presented with good results showing two distinct options. In the first option the patch thickness is varied continuously to provide a reduced and uniform adhesive stress distribution while still maintaining the same load transfer to the patch. In the second, for a given patch design, the adhesive thickness is varied continuously to give a reduced and uniform adhesive stress distribution while still effectively reducing stress in the reinforced component.

It is considered that a number of extensions to the work are warranted. Firstly, it is believed that there is significant scope to change key parameters in the algorithm procedure to reduce the number of iterations required, if desired. Secondly, the approach seems directly applicable to three dimensional geometries.

8. References

1. **HAUG, E.J., CHOI, K.K. and KOMKOV, V.**, *Design Sensitivity Analysis of Structural Systems*, Academic Press Inc, 1986.

2. **FANNI, M., SCHNACK, E. and GRUNWALD, J.**, *Shape Optimisation of Dynamically Loaded Machine Parts*, Vol 59, pp. 281-297, International Journal of Pressure Vessels and Piping, 1994.

3. **FRANCAVILLA, A., RAMAKRISHNAN, C.V. and ZIENKIEWICZ, O.C.**, *Optimisation of Shape to Minimise Stress Concentration*, Vol 10, No 2, Journal of Strain Analysis, 1975.

4. **KRISTENSEN, E.S. and MADSEN, N.F.**, *On the Optimum Shape of Fillets in Plates Subjected to Multiple In-Plane Loading Cases*, Vol 10 1007-1019, International Journal for Numerical Methods in Engineering, 1976.

5. **VANDERPLAATS, G.N.**, 'Numerical Optimisation Techniques for Engineering Design: With Applications' ISBN 0-07-066964-3, McGraw-Hill, 1994.

6. **SCHNACK, E. and SPORL, U.**, 'A Mechanical Dynamic Programming Algorithm for Structure Optimisation', Vol 3, No 11, International Journal for Numerical Methods in Engineering, 1986.

7. **SCHNACK, E.**, *An Optimisation Procedure for Stress Concentrations by the Finite Element Technique*, Vol 14, pp. 115-124, International Journal for Numerical Methods in Engineering, 1979.

8. **MATTHECK, C. and BURKHARDT, S.**, *A New Method of Structural Shape Optimisation Based on Biological Growth*, Vol 12, No 3, International Journal of Fatigue, 1990.

9. **MATTHECK, C., BAUMGARTNER, A. and WALTHER, F.**, *Optimisation Procedures by use of the Finite element Method*, PD-Vol 64-4, Medical and Biological Engineering and Computing, July 1992.

10. **MATTHECK, C., ERB, D., BETHGE, K. and BEGEMANN, U.**, *Three-Dimensional Shape Optimisation of a Bar with a Rectangular Hole*, Vol 15, No 4, pp. 347-351, Fatigue Fract. Engng. Struct., 1992.

11. **ROZVANY, G.I.N., BENDSOE, M.P. and KIRSCH, U.**, *Layout Optimisation of Structures*, Vol 48 No 2, Applied Mechanics Review, 1995.

12. **BENDSOE, M.P.**, 'Optimisation of Structural Topology Shape and Material', ISBN 3-540-59057-9, Springer-Verlag, 1995.

13. **XIE, Y.M. and STEVEN, G.P.**, *A Simple Evolutionary Procedure for Structural Optimisation*, Vol 49, pp. 885-896, Computers and Structures, 1993.

14. **WHEELER, L.**, *On the Role of Constant-Stress Surfaces in the Problem of Minimising Elastic Stress Concentration*, Vol 1-2, pp. 779-789, International Journal of Solids Structures, 1976.

15. **KEAYS, R.H., MOLENT, L. and GRAHAM, A.D.**, *F-111 Wing Pivot Fitting: Finite Element Analysis of Fuel Flow Hole #13*, ARL-STRUCT-TM-557, Aeronautical Research Laboratory, Melbourne, Victoria, July 1992.

16. **OJALVO, I.U.**, *Optimisation of Bonded Joints*, Vol 23, No 10, p. 1578, AIAA Journal, January 1985.

17. **TRAN-CONG, T. and HELLER, M.**, *Reduction in adhesive shear stresses at the ends of bonded reinforcements*, DSTO, AMRL Research Report, Australian Department of Defence, File M1/1/109, 1997.

18. **STIMSON M.G.**, 'FS470.5 *Bulkhead lower centreline crotch - design analysis of the boron doubler*, AMRL IFOSTP document, Department of Defence, File No. 8006000, Ref. No. MGS96006, 4 April 1996.

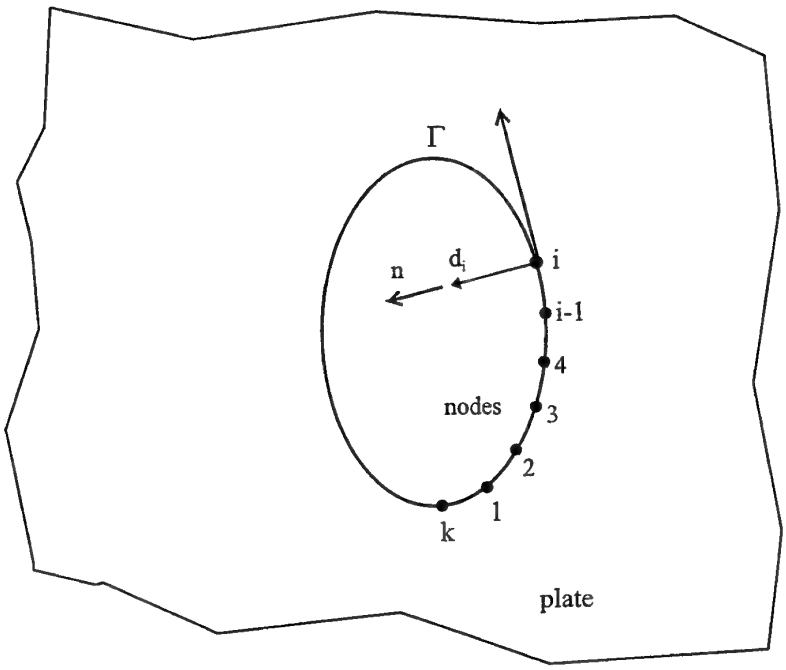

Figure 1. Geometry and notation for an open hole in a remotely loaded plate with boundary shape defined by k nodes on contour Γ.

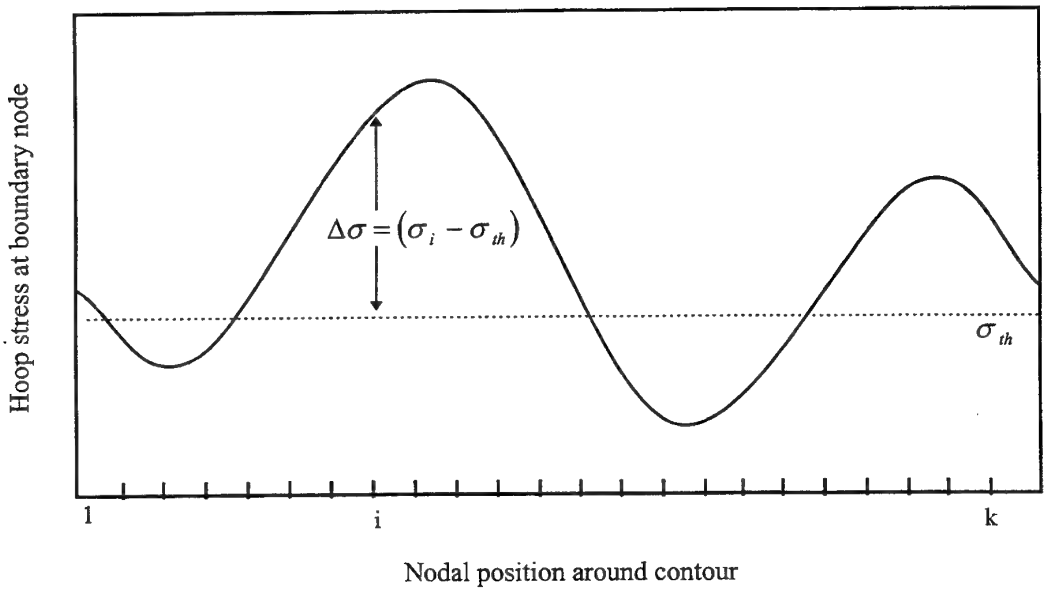

Figure 2. Typical tangential stress distribution around hole boundary contour for remotely loaded plate.

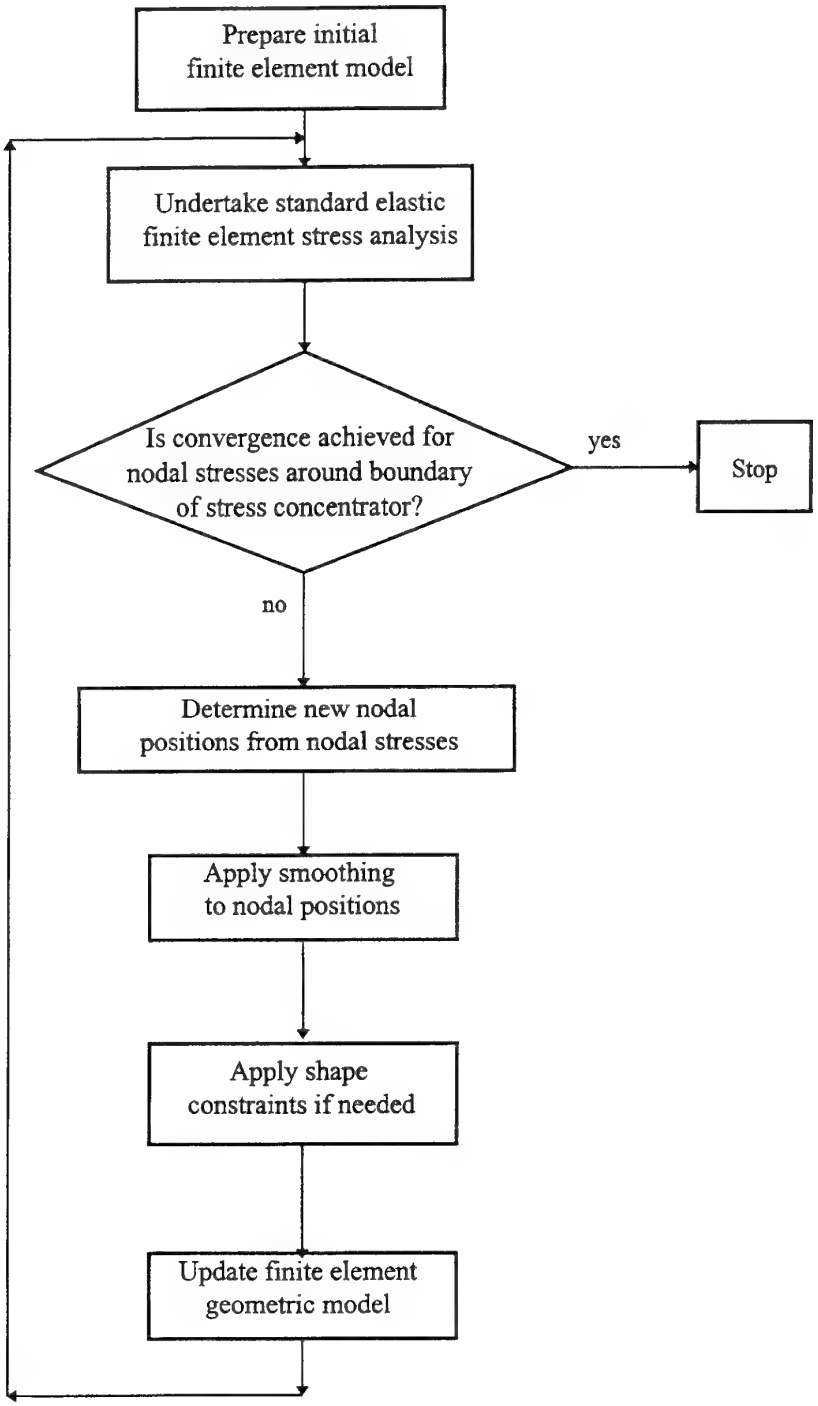

Figure 3. Flowchart for implementation of moving boundary method with standard finite element analysis.

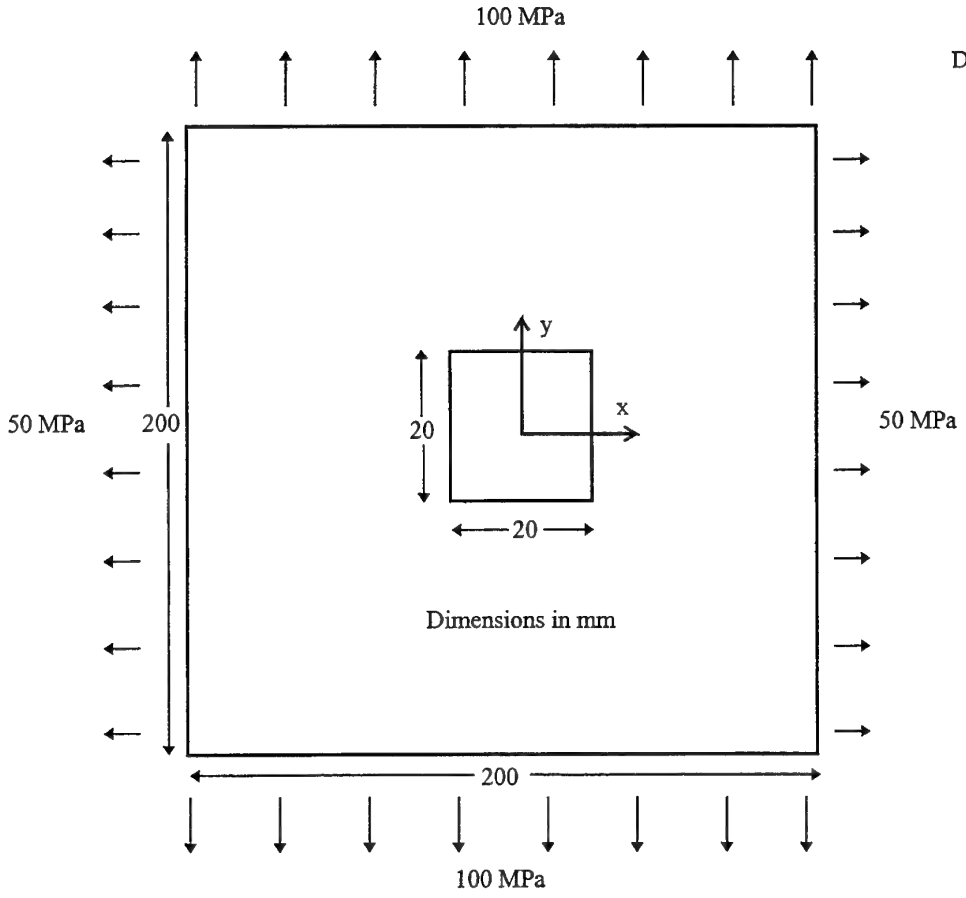

Figure 4. Geometry and loading arrangement for a large square plate containing a square hole with a remote 2:1 biaxial stress field.

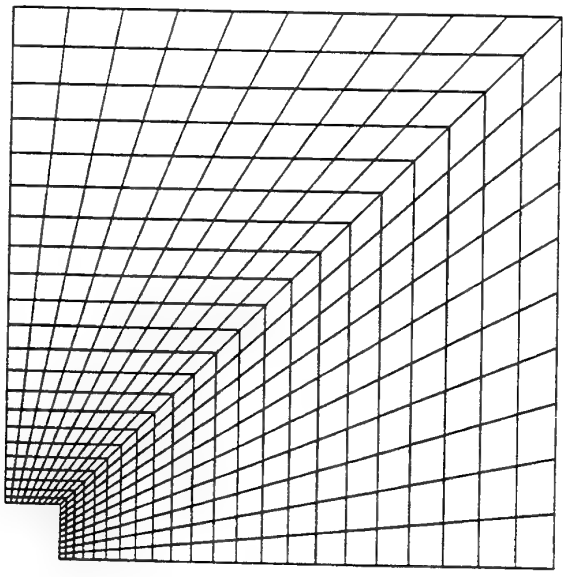

Figure 5. Finite element mesh for modelling a large square plate containing a square hole.

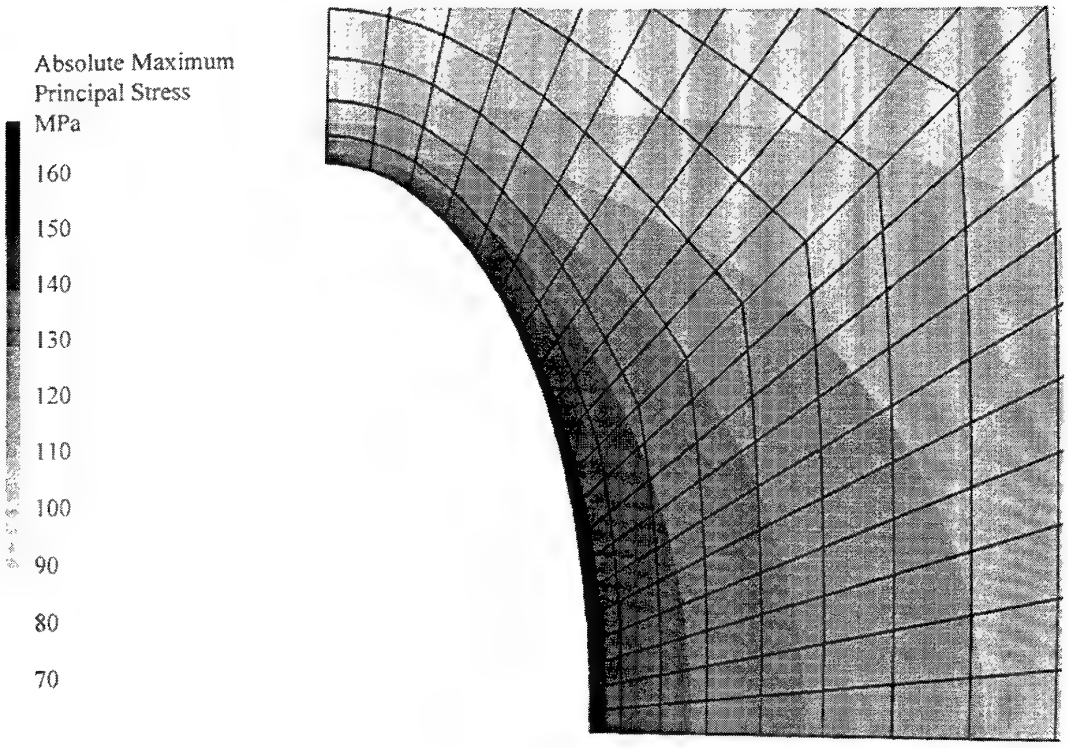

Figure 6. Final shape for problem of optimisation of an initial square hole in a large plate with a remote 2:1 biaxial stress field, showing distribution of maximum principal stress.

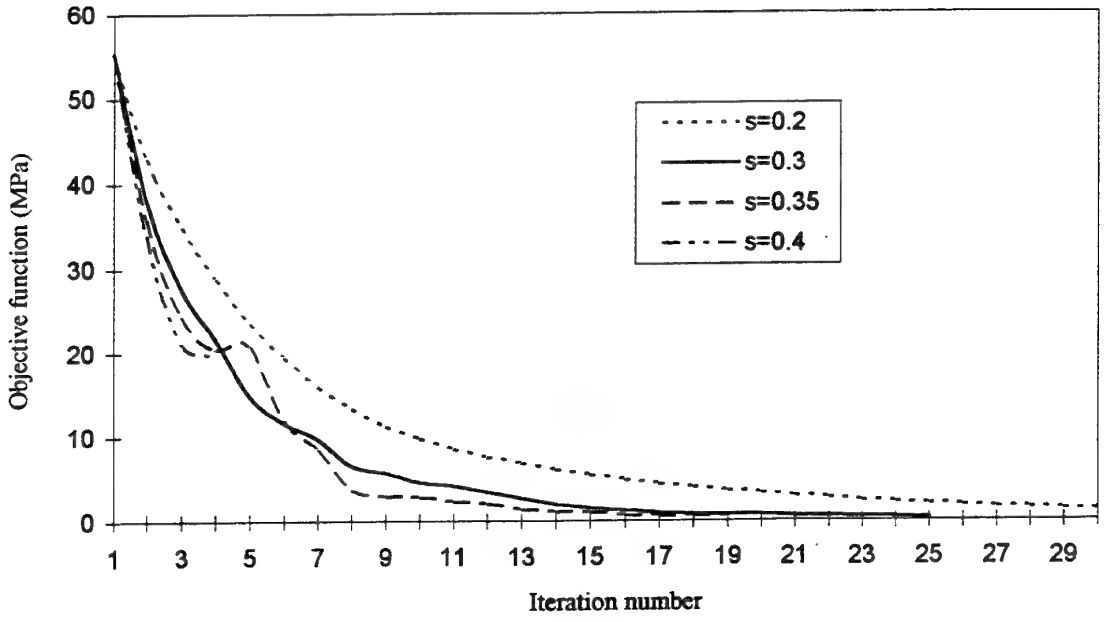

Figure 7. Convergence of objective function for various step factors for a large plate containing an initial square hole with a remote 2:1 biaxial stress field.

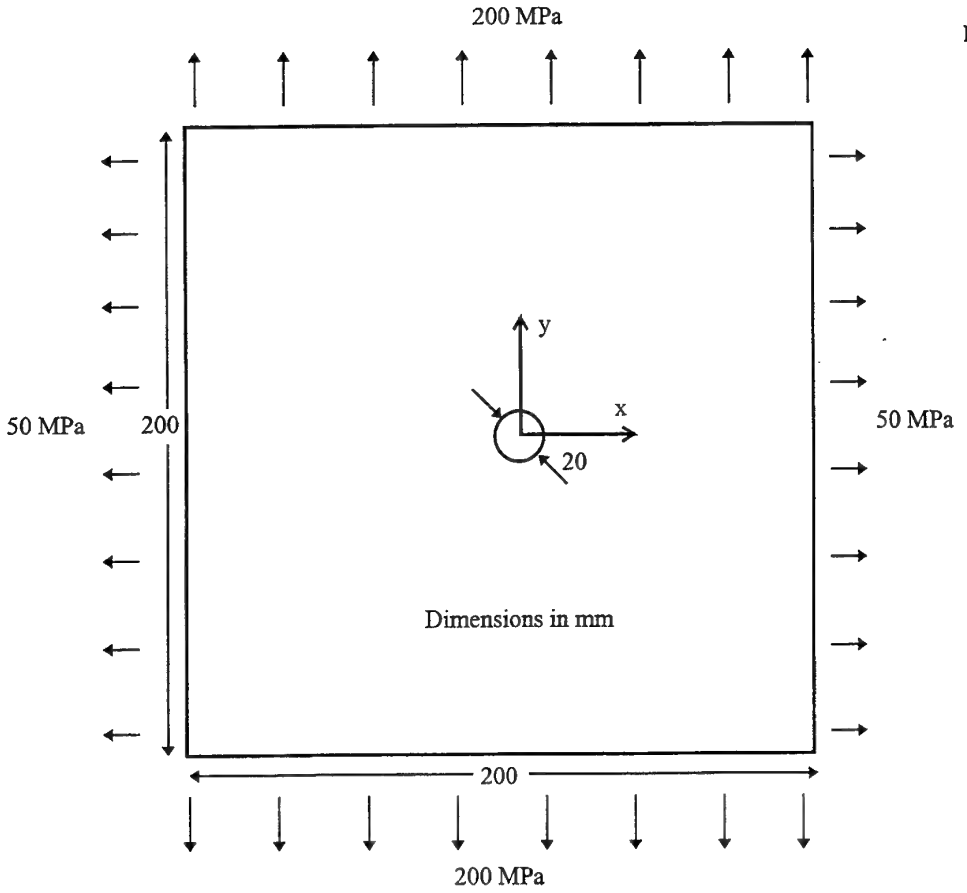

Figure 8. Geometry and loading arrangement for a large square plate containing a round hole with a remote 4:1 biaxial stress field.

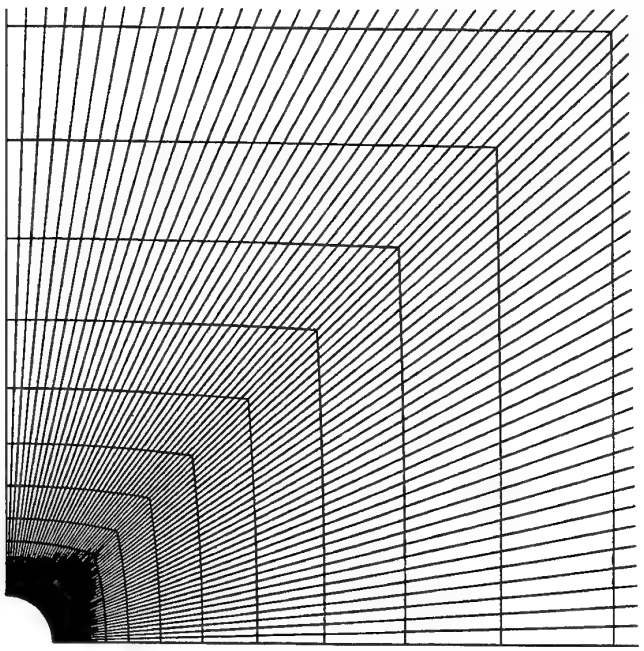

Figure 9. Finite element mesh for modelling a large square plate containing a round hole.

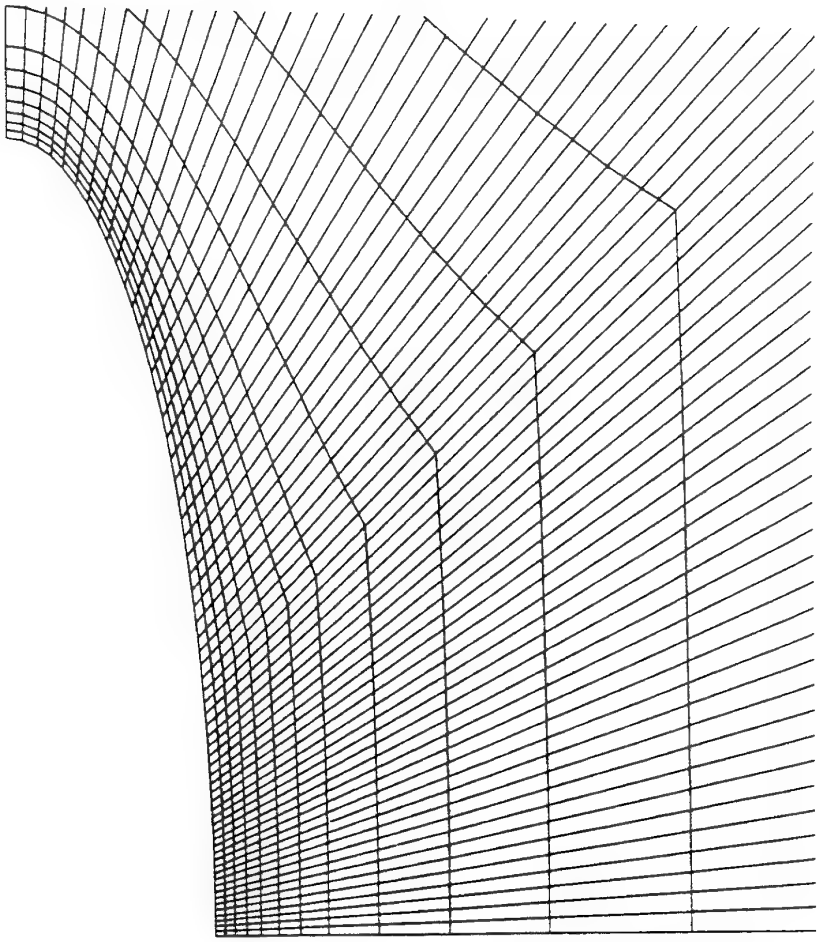

Figure 10. Final hole shape for problem of optimisation of an initial round hole in a large plate with a remote 4:1 biaxial stress field.

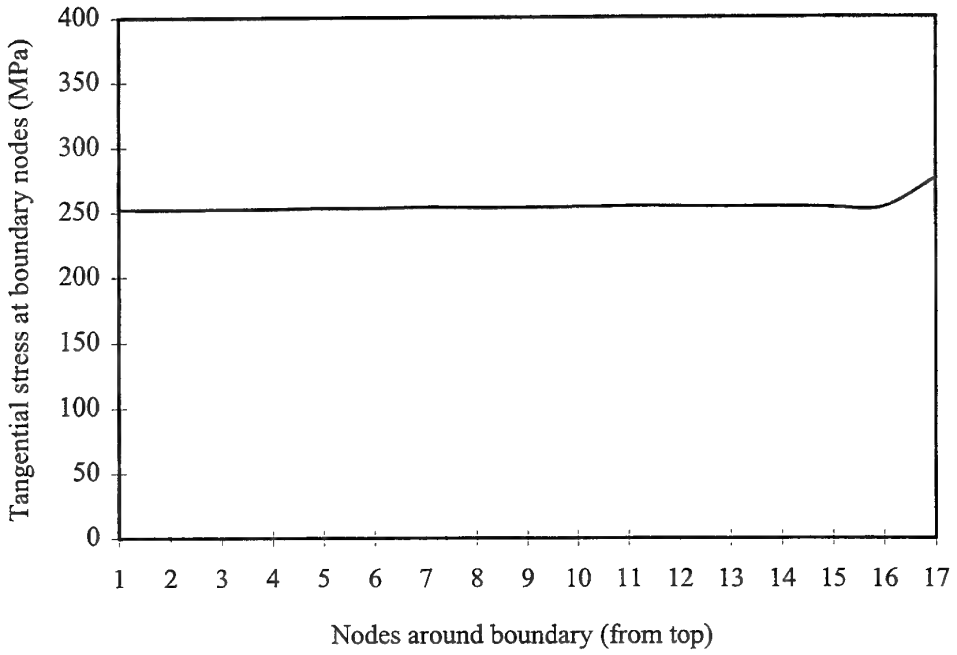

Figure 11. Distribution of tangential stress around hole boundary of final shape for initial round hole in a large plate with a remote 4:1 biaxial stress field

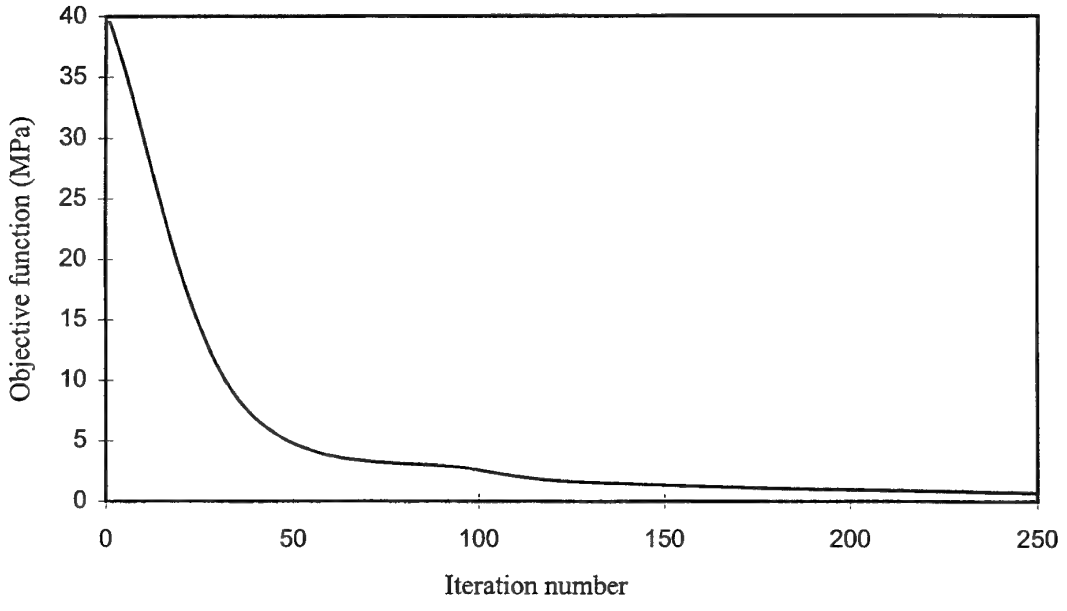

Figure 12. Convergence of objective function for a large plate containing an initial round hole with a remote 4:1 biaxial stress field.

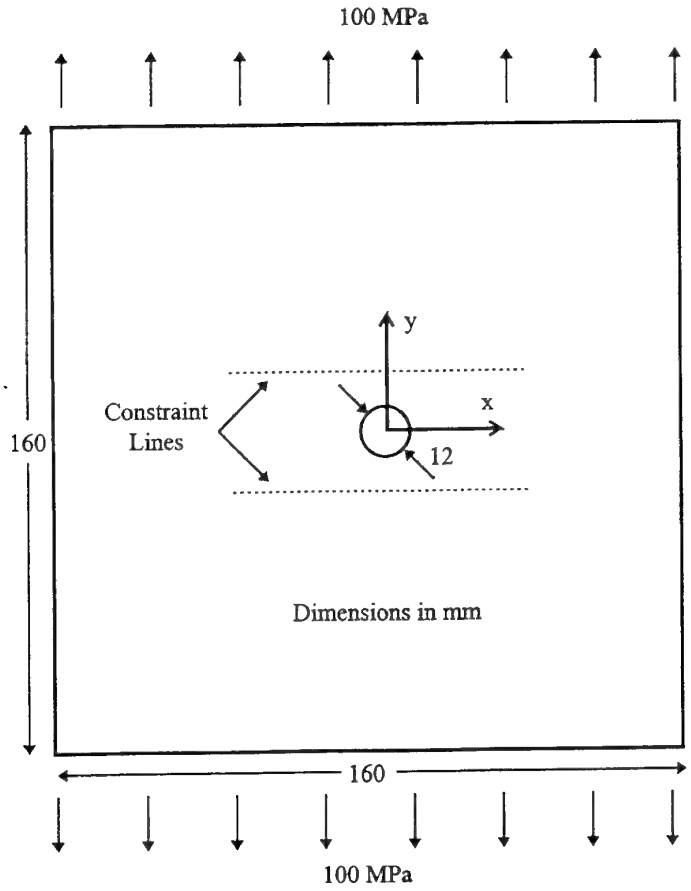

Figure 13. Geometry and loading arrangement for a large square plate containing a round hole with a remote uniaxial applied stress.

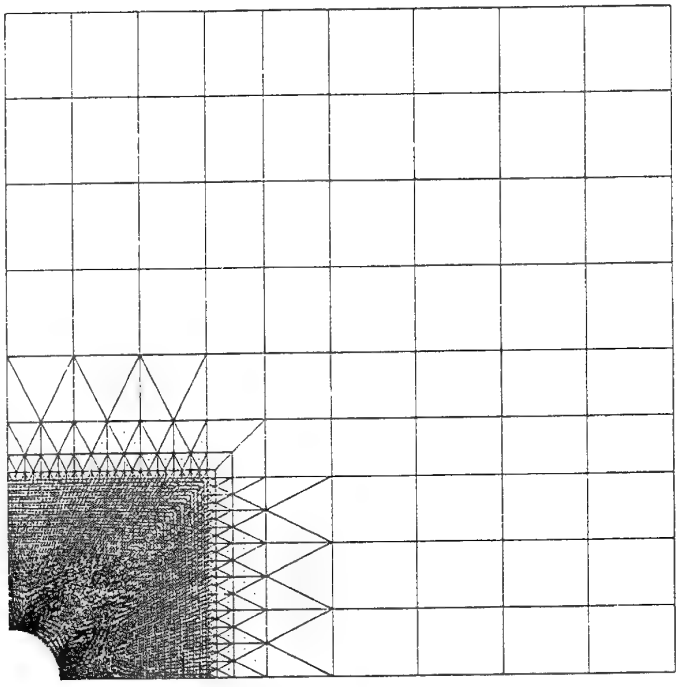

Figure 14. Finite element mesh for modelling a large square plate containing a round hole.

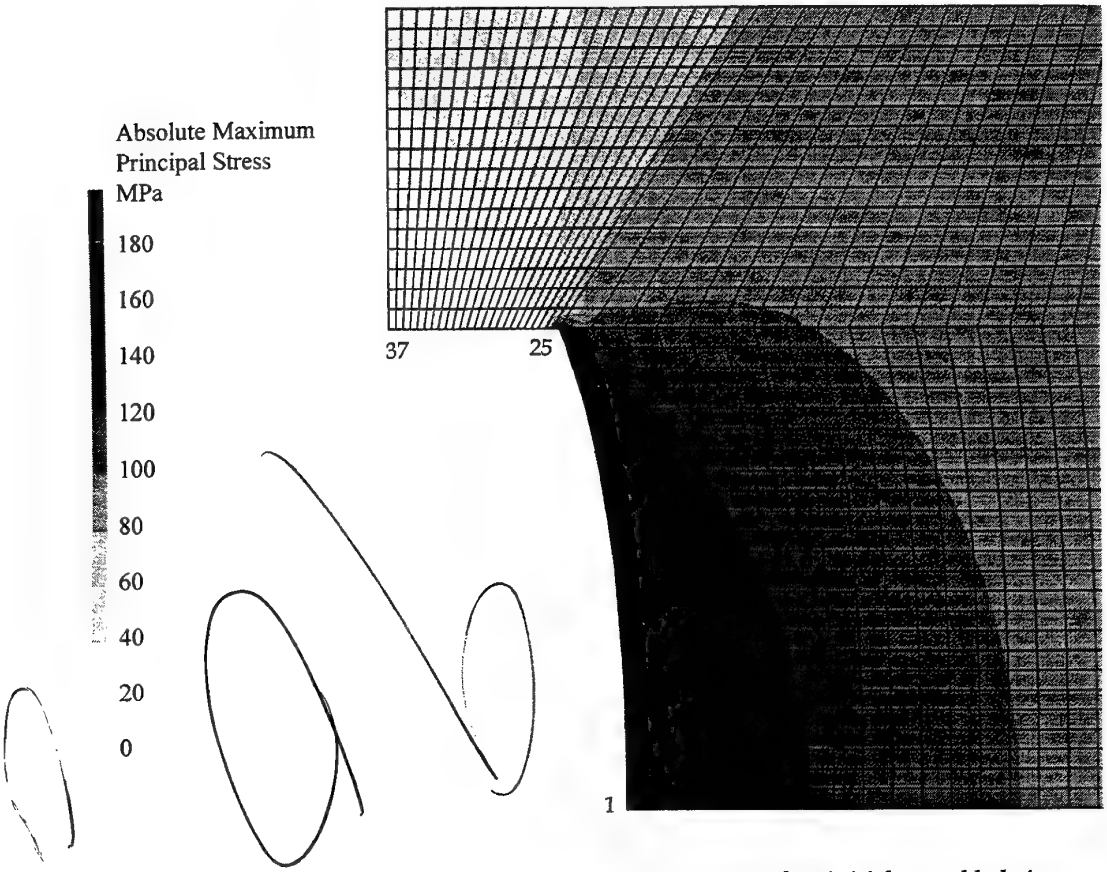

Figure 15. Final shape for problem of constrained optimisation of an initial round hole in a large uniaxially loaded plate, showing distribution of maximum principal stresses.

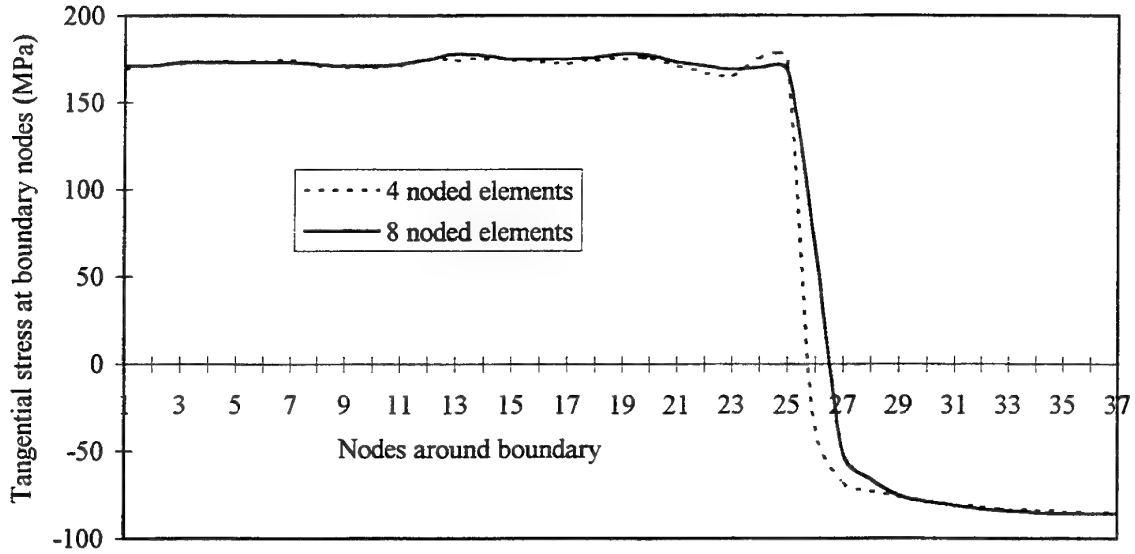

Figure 16. Distribution of tangential stress around hole boundary of final shape for initial round hole in a large uniaxially loaded plate.

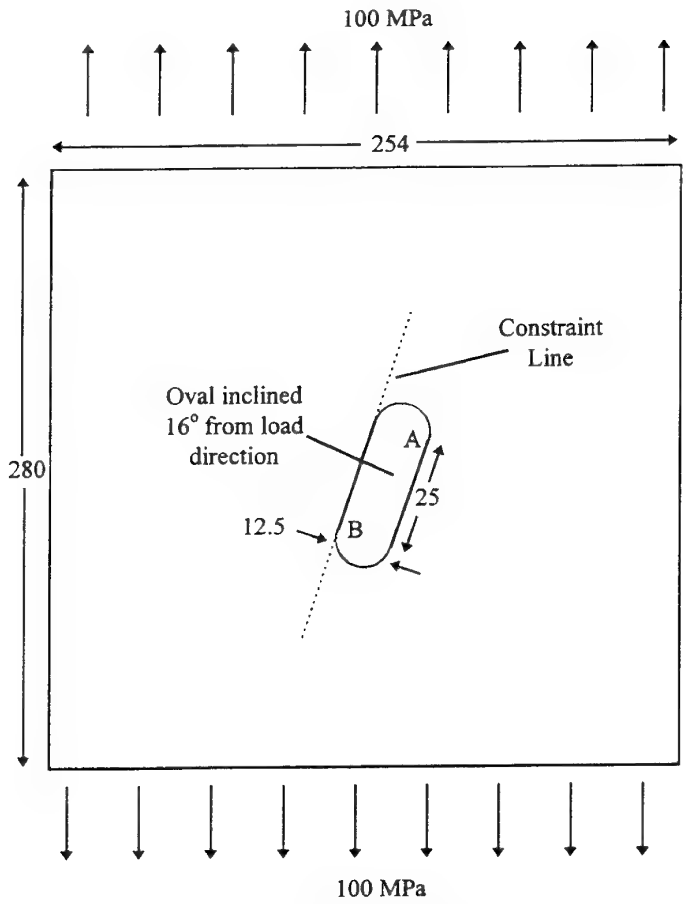

Figure 17. Geometry and loading arrangement for a large rectangular plate containing an inclined oval shaped hole with a remote uniaxial applied stress.

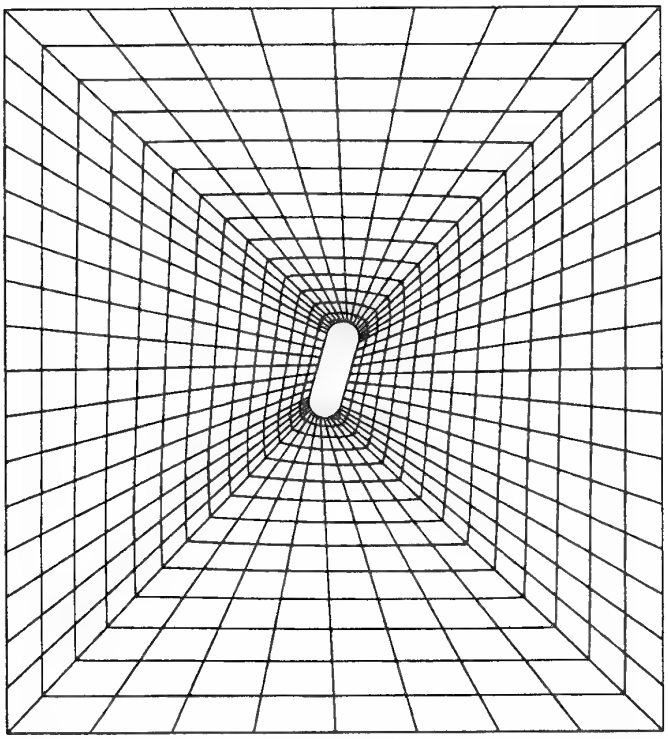

Figure 18. Finite element mesh for a large rectangular plate containing an inclined oval shaped hole with a uniaxial applied stress.

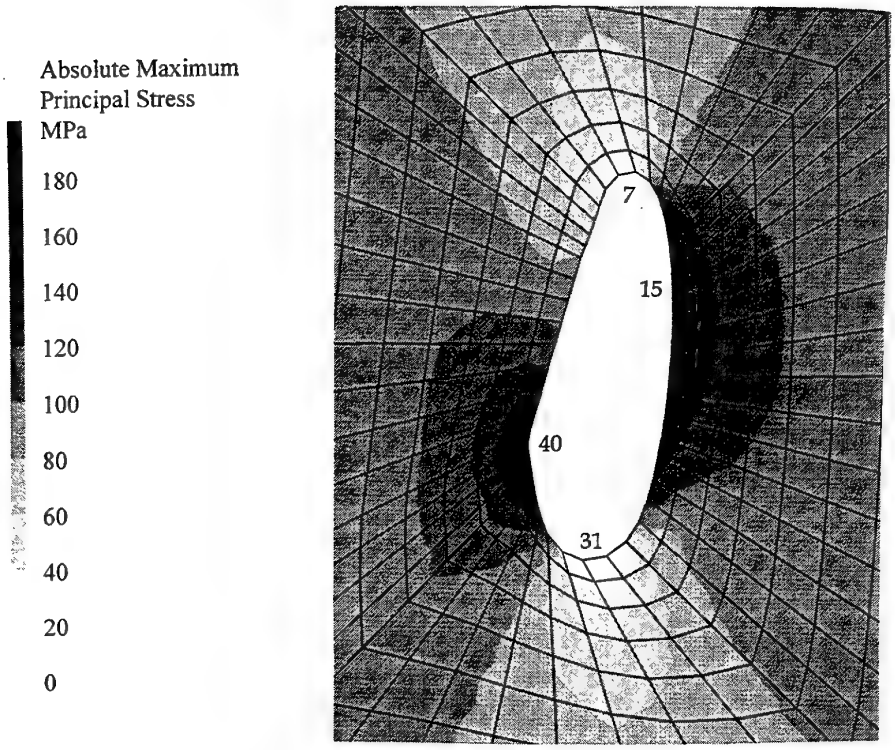

Figure 19. Final shape for problem of constrained optimisation of an initial inclined oval hole in a large uniaxially loaded plate, showing distribution of maximum principal stresses.

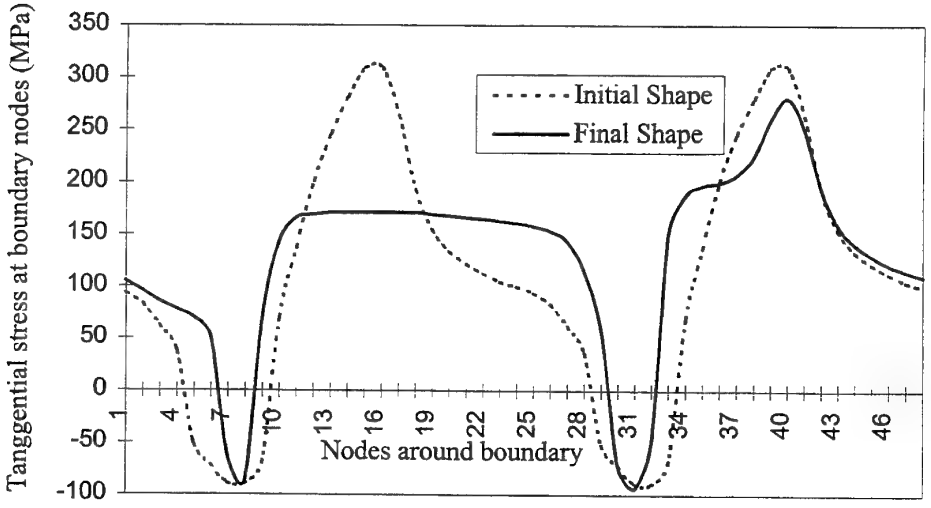

Figure 20. Distribution of tangential stress around hole boundary of final shape for constrained optimisation of an initial inclined oval hole in a large uniaxailly loaded plate.

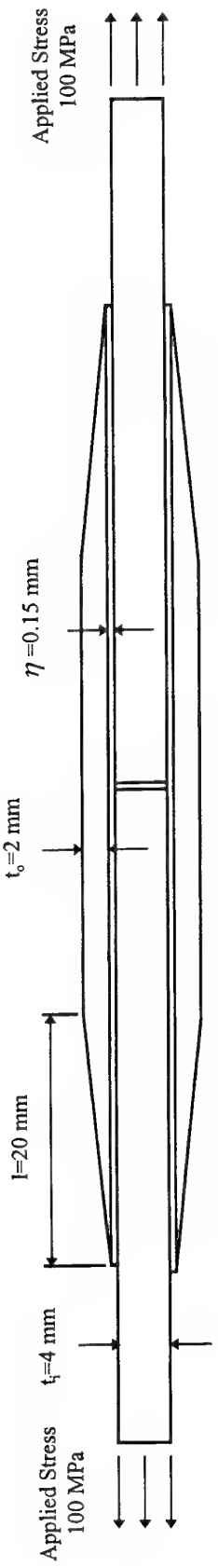

Figure 21. Geometry and loading arrangement for a uniaxially loaded adhesively bonded double lap-joint, showing initial linear taper profile of outer adherend (patch).

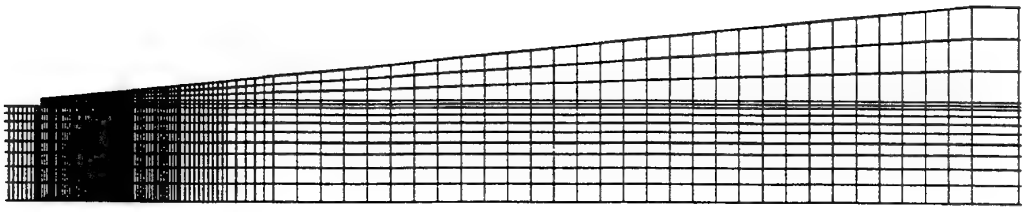

Figure 22(a). Finite element mesh for bonded double lap-joint with initial linear taper profile for patch (only region near taper shown).

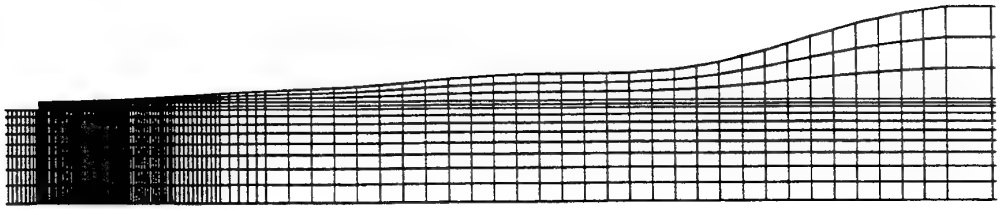

Figure 22(b). Final shape for optimisation of the tapered region of patch for bonded double lap-joint (only region near taper shown).

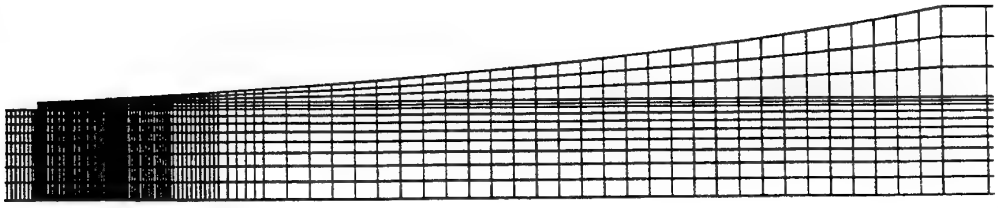

Figure 22(c). Finite element mesh for bonded double lap-joint with patch taper as given by one dimensional analytical solution [16] (only region near taper shown).

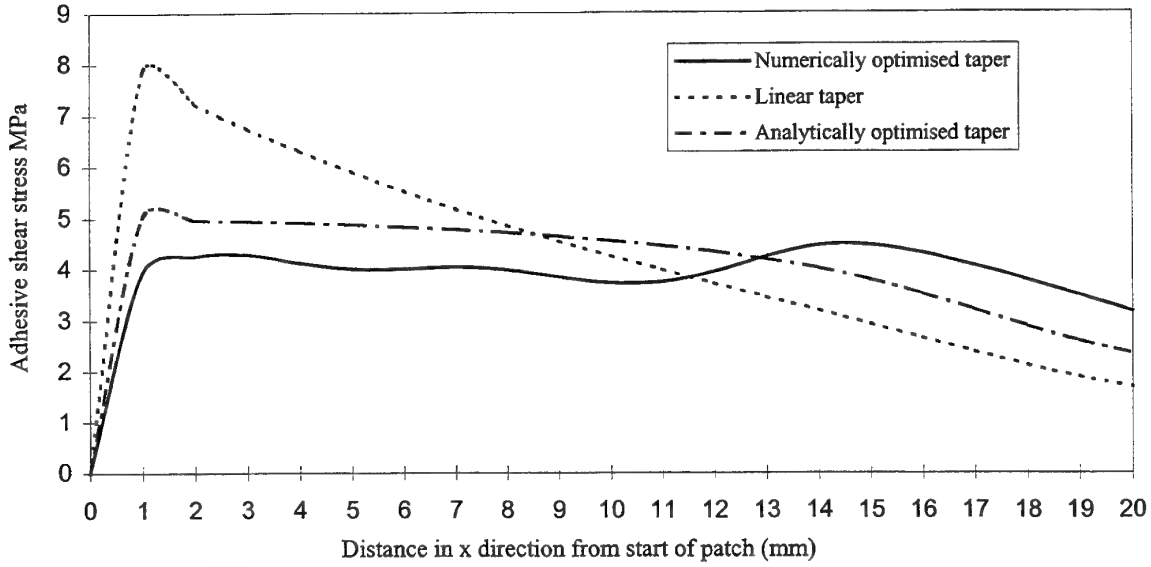

Figure 23. Adhesive shear stress distributions for a bonded double lap-joint with a unidirectional applied stress, for various taper profiles (in taper region only).

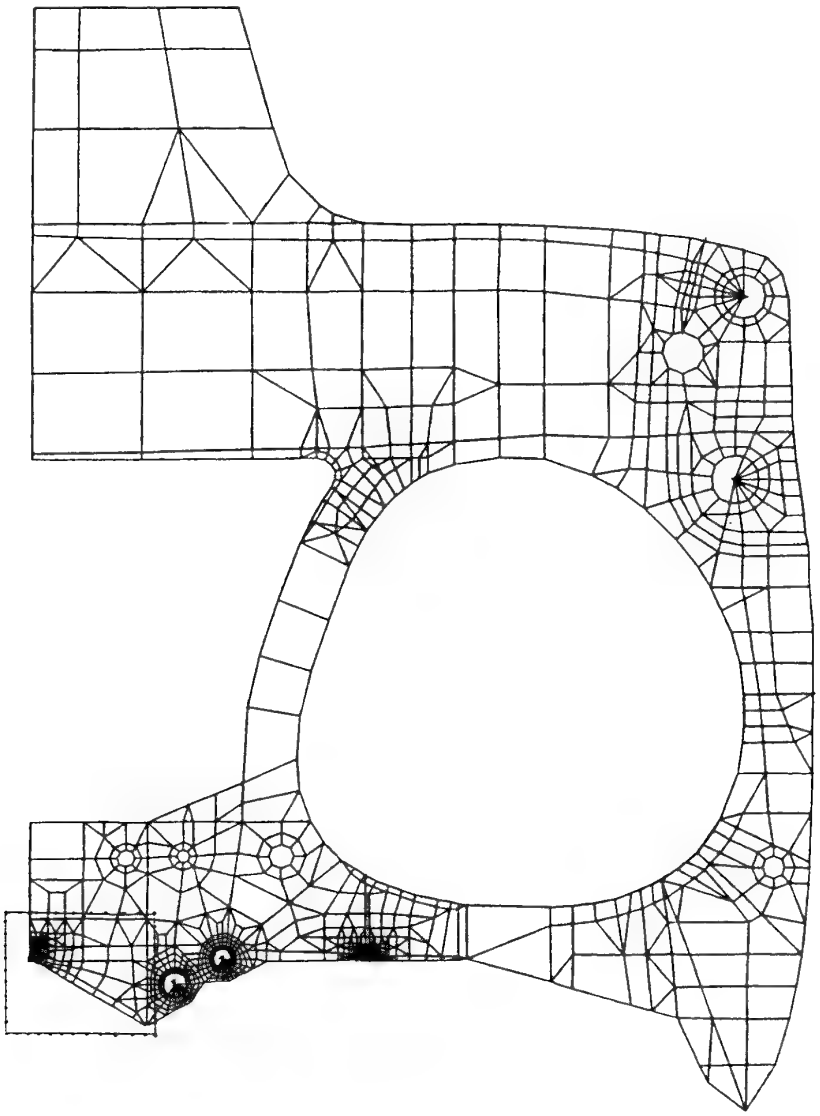

Figure 24. Two dimensional semi-symmetric finite element model of F/A-18 470 bulkhead showing region of substructure.

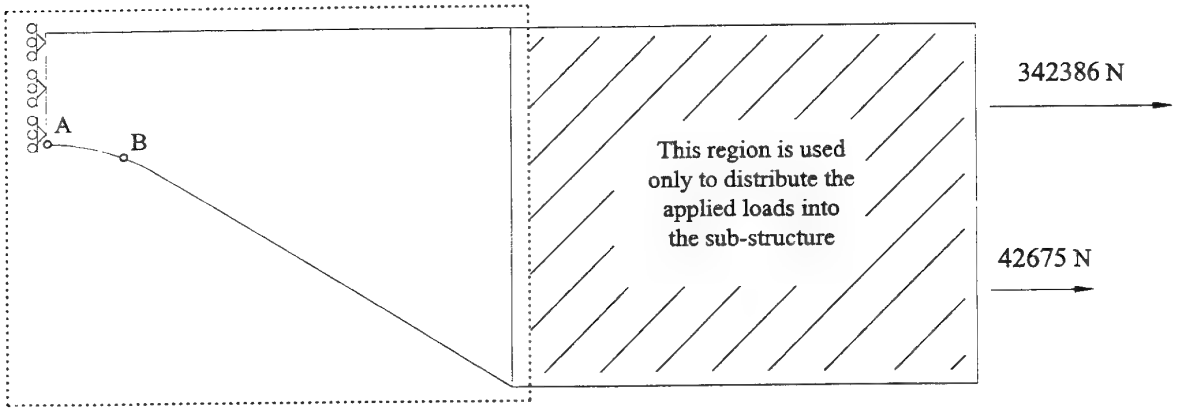

Figure 25. Geometry and loading arrangement for semi-symmetric sub-structure of F/A-18 470 bulkhead.

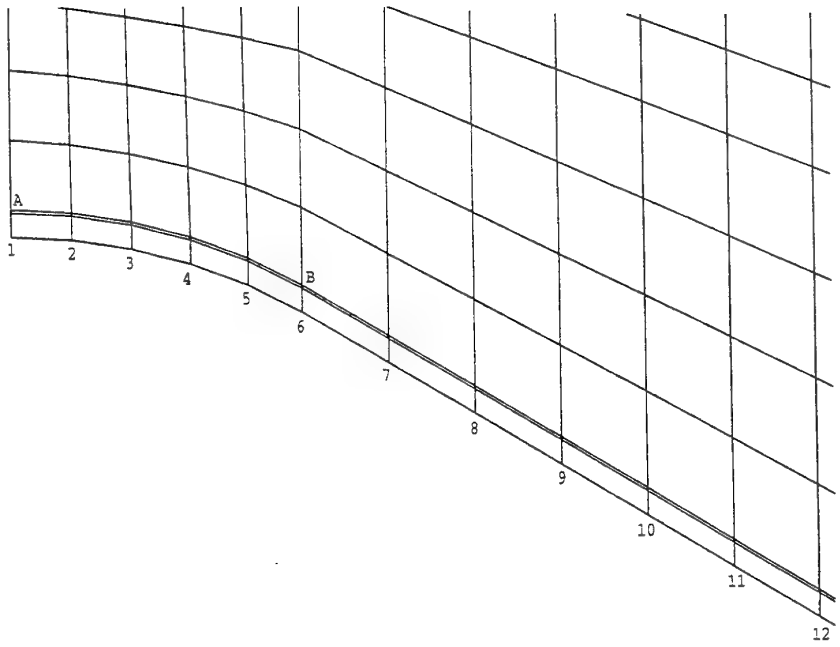

Figure 26. Finite element mesh for critical region of F/A-18 470 bulkhead sub-structure for nominal 8 layer bonded patch with stress reduction at point A of 34%.

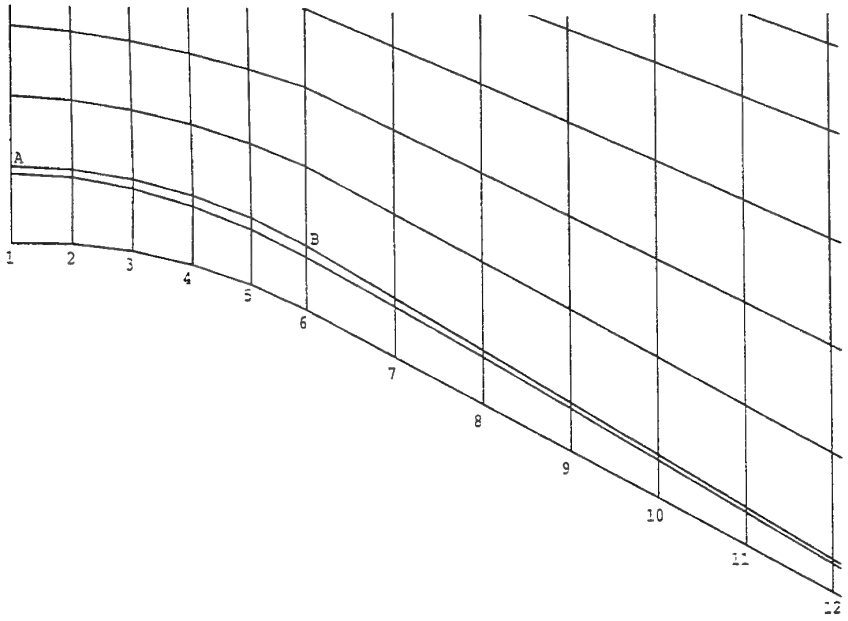

Figure 27. Finite element mesh for critical region of F/A-18 470 bulkhead sub-structure for optimised patch with stress reduction at point A of 42%.).

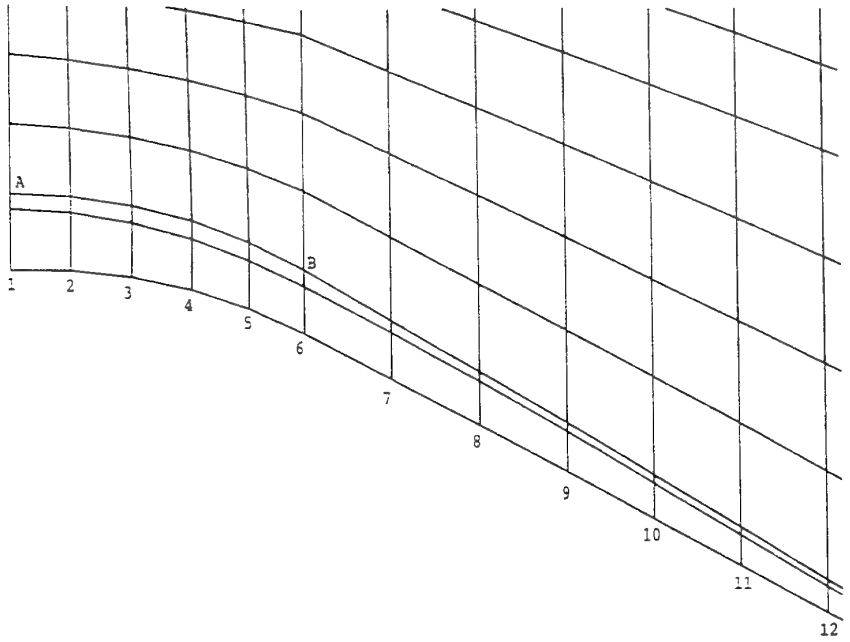

Figure 28. Finite element mesh for critical region of F/A-18 470 bulkhead sub-structure for optimised patch with stress reduction at point A of 34%.

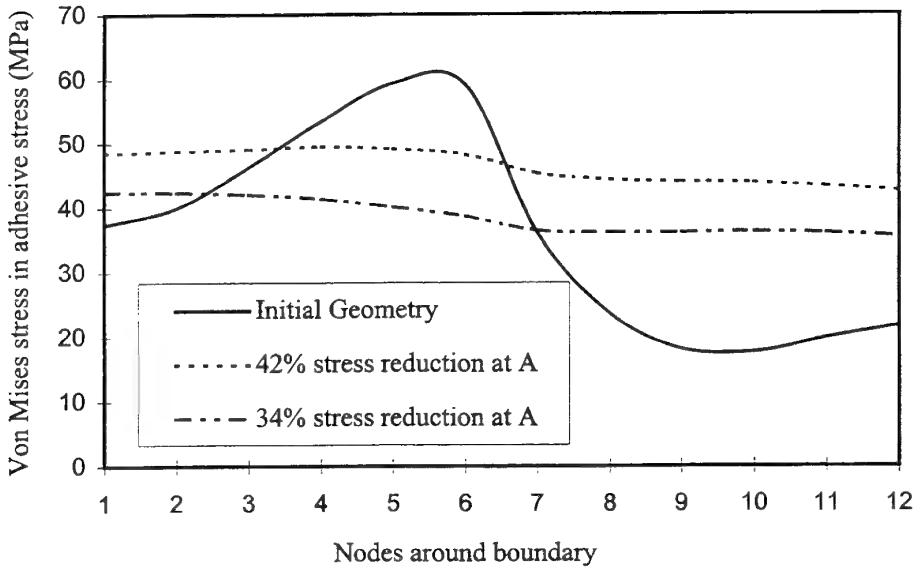

Figure 29. Comparison of von Mises adhesive stress distributions for F/A-18 470 bulkhead sub-structure region with initial and optimised bonded patches.

9. Appendix A: Implementation of Moving Boundary Method In PAFEC Finite Element Code

9.1 General comments

The implementation of the moving boundary node method with PAFEC is described by the flow chart given in Figure A.1. The finite element software is used to solve for the stresses at each iteration with the finite element model constructed such that the boundary nodes to be moved are corners of PAFEC PAFBLOCKS. PAFBLOCKS are a geometric entity that contain proportional iso-meshing of finite elements within. A new PAFBLOCK corner position leads to new positions of all the internal nodes that maintain the original mesh proportions. It is advantageous in some cases to select the initial shapes of the PAFBLOCKS such that the new corner positions will not cause any elements to become badly distorted as the iteration process proceeds.

The initial model is prepared in the normal way using the operating system and a text editor. Overall aspects of the process such as the iterations and file handling are controlled by a UNIX shell script which is given in section 9.2. Convergence checking and node movements are performed by a FORTRAN program which is executed by the shell script. The FORTRAN program needs to be modified slightly for different problems. Changes mostly relate to the method used to calculate the direction of node movements, and three point smoothing for various levels of symmetry.

A dedicated directory is preferred for each problem due to the amount of file handling performed by the shell script and the PAFEC solution. The primary output is a log file containing mainly stresses and nodal coordinates for each iteration. The PAFEC binary file containing the mesh and model description is also retained so that any of the shape variations can be plotted. A second shell script is used to delete and initialise files for restarting the problem.

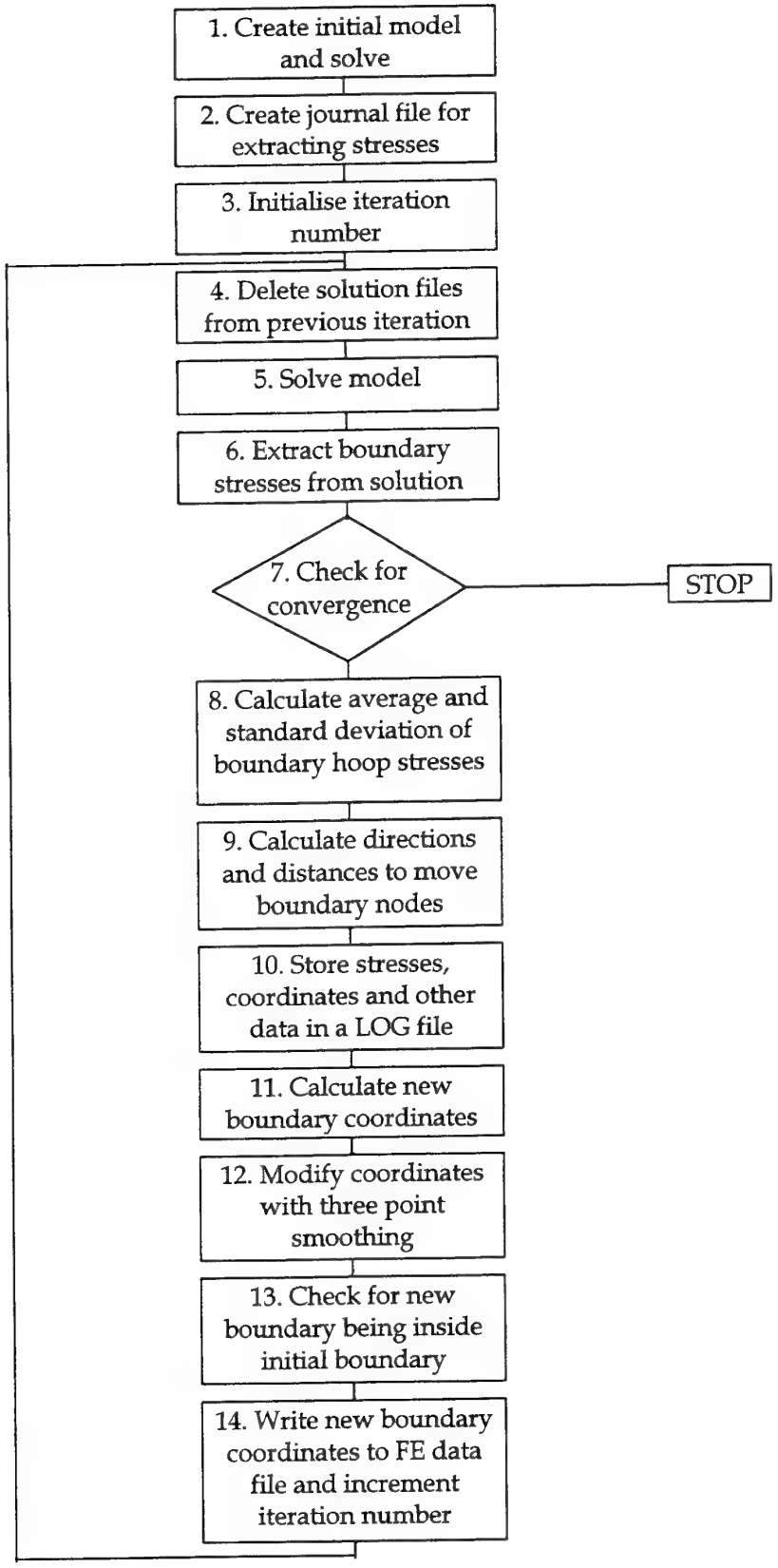

Figure A.1 - Flow chart for implementation of the moving boundary node method with PAFEC finite element code

9.2 Unix shell script for controlling iterations

```
maxcount="31"

read jobname < JNAME.DAT
count="1"
#
until [ $count = $maxcount ]
do
  echo $count
  pafdel $jobname
  pafrun $jobname
  cp $jobname".BS" $jobname$count".BS"
  pupname="PUP.JNL"
  echo $pupname
  pup $pupname
  mn
#
#    Terminate job on Solution solved
#
   if [ -f JOB.SOLVED ]; then
     break
   fi
   count=`expr $count + 1`
done
```

9.3 Fortran program for moving nodes

```
program movenodes

C This is the version of code used for the analysis presented in section 4.2.
C Here it is assumed that the problem domain is in the first quadrant and the
C plate geometry is quarter symmetric.

C Declarations
      implicit  none
      logical   solved
      character aline*80,jobname*10,filename*20
      integer   eofn,i,j,k,ios,n,nodes,joblen,linelen
      real      rnum,x,y,z,s1,s2,s3,th1,th2,th3,pi
      real      hoop,hooptot,avhoop,r,th,d,h,dhoop,vartot,
                variance
      character chr
      dimension n(40,20),x(40,20),y(40,20),z(40,20),hoop(40,20),
      th(40,20),d(40,20),s1(40,20),s2(40,20),s3(40,20),th1(40,20),
     *th2(40,20),th3(40,20),variance(20),avhoop(20)


C Read in iteration number
      open (unit=10,file='ITNUM.DAT')
      read(10,235) j
  235 format(i2)
      close(10)


C Open PUPPIES output file
      filename='JOB.PUPPIES'
      open (unit=20,file=filename,err=1010,status='old')

C Read through alphajunk to find first line of numeric data
```

```
C (i.e. nodal coordinates)
      ios=1
      do while (ios.ne.0)
       read(20,*,iostat=ios) rnum
      end do
      backspace(20)

C Read in node numbers and coordinates
      i=0
      do while (ios.eq.0)
       i=i+1
       read(20,*,iostat=ios) n(i,j), x(i,j), y(i,j), z(i,j)
      end do
      nodes=i-1

C Read through more alphajunk to find first line of stress data
      ios=1
      do while (ios.ne.0)
       read(20,*,iostat=ios) rnum
      end do
      backspace(20)

C Read in stresses and directions
      i=0
      do while (ios.eq.0)
       i=i+1
       read(20,*,iostat=ios) n(i,j),s1(i,j),s2(i,j),
     * s3(i,j),th1(i,j),th2(i,j),th3(i,j)
      end do
      close(20)

C If this is not the first iteration get the results of previous
C iterations from the log file JOBOPT.LOG
      if (j.gt.1) then
       k=j
       open (unit=10,file='JOBOPT.LOG',status='old')
       do j=1,k-1
        read(10,*,iostat=ios) rnum
        read(10,*,iostat=ios) avhoop(j)
        read(10,*,iostat=ios) variance(j)
        read(10,*,iostat=ios) rnum
        do i=1,nodes
         read(10,*,iostat=ios) n(i,j),x(i,j),y(i,j),s1(i,j),s2(i,j),
     *   th1(i,j),th2(i,j),th(i,j),d(i,j)
        end do
       end do
       j=k
      end if
      close(10)

C Store hoop stresses in array hoop and calculate average hoop stress
      hooptot=0
      do i=1,nodes
       if (abs(s1(i,j)).gt.abs(s2(i,j))) then
        hoop(i,j)=s1(i,j)
       else
        hoop(i,j)=s2(i,j)
       end if
       hooptot=hooptot+hoop(i,j)
      end do
      avhoop(j)=hooptot/nodes

C Calculate variance
      vartot=0
      do i=1,nodes
```

```
       vartot=vartot+(hoop(i,j)-avhoop(j))**2
      end do
      variance(j)=sqrt(vartot/avhoop(j))
C Calculate base length
C     r=sqrt(x(1,j)**2+y(1,j)**2)
      r=6


C Calculate the direction to move nodes (clockwise from y axis)
      pi=3.14159
      do i=1,nodes
       if (i.eq.1) th(i,j)=0
       if (i.gt.1.and.i.lt.nodes) then
        h=sqrt((x(i+1,j)-x(i-1,j))**2+(y(i+1,j)-y(i-1,j))**2)
        th(i,j)=asin((y(i+1,j)-y(i-1,j))/h)
        th(i,j)=-th(i,j)
       end if
       if (i.eq.nodes) th(i,j)=pi/2
      end do

C  Now calculate d, the distance to be moved and check for convergence
      solved=.true.
      do i=1,nodes
        dhoop=(avhoop(j)-hoop(i,j))/avhoop(j)
        d(i,j)=dhoop*r*0.7
        if (abs(dhoop).gt.0.02) solved=.false.
      end do

C Write LOG file to JOBOPT.LOG
      filename='JOBOPT.LOG'
      open (unit=30,file=filename)
      k=j
      do j=1,k
       write(30,*) j,' = iteration number'
       write(30,*) avhoop(j),' = average hoop stress'
       write(30,*) variance(j),' = Variance '
       write(30,*) 'NODE    X       Y       S1      S2'//
     * '     th1     th2     th(i)   d(i)'
       do i=1,nodes
        write(30,220) n(i,j),x(i,j),y(i,j),s1(i,j),s2(i,j),
     *  th1(i,j),th2(i,j),th(i,j),d(i,j)
  220   format(i3,8f8.2)
       end do
      end do
      j=k
      close(30)

      if (solved) then
       open(unit=30,file='JOB.SOLVED')
       close(30)
       stop
      end if

C  Change coordinates
      do i=1,nodes
        if (d(i,j).gt.0) then
         x(i,j)=x(i,j)+d(i,j)*sin(th(i,j))
         y(i,j)=y(i,j)+d(i,j)*cos(th(i,j))
        end if
      end do

C Make copy of pafec data file in TEMP.DAT
      filename='JOB.DAT'
      open (unit=30,file=filename,err=1020,status='old')
      open (unit=40,file='TEMP.DAT')
```

```
      ios=0
      do while (ios.eq.0)
       read(30,210,iostat=ios,end=1030) aline
  210  format(a80)
       call jplen(aline,i)
       write(40,*) aline(1:i)
      end do
 1030 continue
      close (30)
      close (40)

C Write new pafec data file with new nodal coordinates added
      filename='JOB.DAT'
      open (unit=30,file=filename)
      open (unit=40,file='TEMP.DAT',err=1040,status='old')
      ios=0
      do while (ios.eq.0)
       read(40,210,iostat=ios,end=1050) aline
       call jplen(aline,linelen)
       call pulstrip(aline,linelen)
        if (aline(1:8).eq.'PAFBLOCK') then
         do i=1,nodes
          write(30,225) n(i,j),x(i,j),y(i,j)
  225     format(i3,2f10.3)
         end do
         write(30,215) 'C'
  215    format(a1)
        end if
       write(30,210) aline
      end do
 1050 continue
      close(30)
      close(40)
C Increment iteration number and write to file
      j=j+1
      open(unit=10,file='ITNUM.DAT')
      write(10,235) j
      close(10)

      stop
1010 write(6,*) 'Could not open PUPPIES output file'
      stop
 1020 write(6,*) 'Could not open Pafec data file'
      stop
 1040 write(6,*) 'Could not open TEMP.DAT'
      end
The following subroutines by courtesy of J. Paul AED, AMRL.

SUBROUTINE JPLEN(STRG,ILEN)
C     THIS SUBROUTINE OBTAINS THE LENGTH OF A STRING
C     INPUT:  STRG - STRING TO HAVE LENGTH DETERMINED
C     OUTPUT: ILEN - LENGTH OF STRING
C
      CHARACTER*(*) STRG
C
C-----FIND LENGTH OF STRING.
      ILEN = LEN(STRG)
10    IF (STRG(ILEN:ILEN).EQ.' ') THEN
         ILEN = ILEN - 1
         IF (ILEN.GT.0) GOTO 10
      END IF
C
C-----CHECK FOR FIRST NULL CHARACTER IN CASE THERE ARE ONES
      DO L1=1,ILEN
         N = ICHAR(STRG(L1:L1))
```

```
         IF (N.EQ.0) THEN
            ILEN = L1 - 1
            GOTO 20
         END IF
      END DO
20    CONTINUE
C
      RETURN
      END

      SUBROUTINE PULSTRIP(STRG,ILEN)
C     THIS SUBROUTINE STRIPS LEADING BLANK SPACES FROM A
C     STRING
C     INPUT  STRG - CHARACTER STRING BE STRIPPED
C     OUTPUT ILEN - NUMBER OF CHARACTERS IN STRING
      CHARACTER*(*) STRG,    CTEMP*300
C
      CTEMP = STRG(1:ILEN)
C
C-----LOOP TO DETERMINE FIRST NON BLANK CHARACTER
      ILOC = 1
10    IF (CTEMP(ILOC:ILOC).EQ.' ') THEN
         ILOC = ILOC + 1
         IF (ILOC.LT.ILEN) GOTO 10
      END IF
C
C-----RE-CONSTRUCT STRING IF BLANK CHARACTERS EXIST
      IF (ILOC.GT.1) THEN
         STRG = CTEMP(ILOC:ILEN)
         ILEN = ILEN - ILOC + 1
      END IF
C
      RETURN
      END
```

9.4 File names and descriptions

JOB.DAT This is the name of the PAFEC data file. A new set of boundary nodes are added to the nodes module at the end of each iteration. Other files of the form JOB.* are created by PAFEC in the process of solving the model and deleted by the PAFDEL routine at the start of the next iteration. It should be noted that PAFDEL is a pre-existing in-house routine for deleting PAFEC output files in preparation for a new PAFEC run.

JOBi.BS These are the PAFEC binary storage files for the model including loads and restraints, where i is the iteration number. For each iteration they are copied from the active JOB.BS. They do not contain stress results. They are saved for later plotting the shape at any iteration.

JOBOPT.LOG Stresses, coordinates and other key quantities for each iteration are stored in this file. It is the best record of the progress of a solution.

PUP.JNL This is a journal file for a data extraction program called PUPPIES. It contains the list of node numbers that are to be moved as well as commands to extract average nodal principal stresses.

JOB.PUPPIES When PUPPIES is executed using the journal file PUP.JNL a list of nodal coordinates and stresses is written to this file. This file is also removed prior to the next iteration. It should be noted that PUPPIES is a pre-existing in-house routine for extracting particular PAFEC output in numeric form.

ITNUM.DAT Contains the iteration number in i2 format.

ITNUM.ONE Is copied to ITNUM.DAT to initialise the iteration number. Contains 1 in same format as above.

SPARE.DAT The initial PAFEC data file is stored here. It is copied to JOB.DAT to re-initialise the model before restarting.

JOB.SOLVED This file is created by the FORTRAN program when convergence is satisfied. The shell script terminates when this file is present in the directory. The file never contains any data.

TEMP.DAT Used for temporary storage of the PAFEC data file JOB.DAT.

9.5 Shell script to prepare files for restarting an optimisation

```
rm JOB*.*
rm *.LOG
rm TEMP.*
cp SPARE.DAT JOB.DAT
cp ITNUM.ONE ITNUM.DAT
F77 mn mn.f
```

mn.f is the fortran program that moves the nodes and is recompiled between runs to incorporate any changes, e.g step size.

DISTRIBUTION LIST

Structural Shape Optimisation by Iterative Finite Element Solution

R. Kaye and M. Heller

AUSTRALIA

1. DEFENCE ORGANISATION

a. Task Sponsor **AIR OIC ASI-LSA**

b. S&T Program

Chief Defence Scientist
FAS Science Policy
AS Science Corporate Management
} shared copy

Director General Science Policy Development
Counsellor Defence Science, London (Doc Data Sheet)
Counsellor Defence Science, Washington (Doc Data Sheet)
Scientific Adviser to MRDC Thailand (Doc Data Sheet)
Director General Scientific Advisers and Trials/Scientific Adviser Policy and Command (shared copy)
Navy Scientific Adviser (Doc Data Sheet and distribution list only)
Scientific Adviser - Army (Doc Data Sheet and distribution list only)
Air Force Scientific Adviser
Director Trials

Aeronautical and Maritime Research Laboratory
Director

Chief of Airframes and Engines Division
Research Leader Fracture Mechanics
Research Leader Aircraft Composite Structures
W. Waldman
R. Evans
R. Kaye (3 copies)
M. Heller (10 copies)

DSTO Library
Library Fishermens Bend
Library Maribyrnong
Library Salisbury (2 copies)
Australian Archives
Library, MOD, Pyrmont (Doc Data sheet only)

c. Capability Development Division
Director General Maritime Development (Doc Data Sheet only)
Director General Land Development (Doc Data Sheet only)
Director General C3I Development (Doc Data Sheet only)

e. **Army**
ABCA Office, G-1-34, Russell Offices, Canberra (4 copies)

g. **Intelligence Program**
Defence Intelligence Organisation
Library, Defence Signals Directorate (Doc Data Sheet only)

i. **Corporate Support Program (libraries)**
OIC TRS, Defence Regional Library, Canberra
Officer in Charge, Document Exchange Centre (DEC), 1 copy
*US Defence Technical Information Centre, 2 copies
*UK Defence Research Information Center, 2 copies
*Canada Defence Scientific Information Service, 1 copy
*NZ Defence Information Centre, 1 copy
National Library of Australia, 1 copy

2. **UNIVERSITIES AND COLLEGES**

Australian Defence Force Academy
Library
Head of Aerospace and Mechanical Engineering
Deakin University, Serials Section (M list), Deakin University Library, Geelong, 3217
Senior Librarian, Hargrave Library, Monash University
Librarian, Flinders University

3. **OTHER ORGANISATIONS**

NASA (Canberra)
AGPS

OUTSIDE AUSTRALIA

4. **ABSTRACTING AND INFORMATION ORGANISATIONS**
INSPEC: Acquisitions Section Institution of Electrical Engineers
Library, Chemical Abstracts Reference Service
Engineering Societies Library, US
Materials Information, Cambridge Scientific Abstracts, US
Documents Librarian, The Center for Research Libraries, US

5. **INFORMATION EXCHANGE AGREEMENT PARTNERS**
Acquisitions Unit, Science Reference and Information Service, UK
Library - Exchange Desk, National Institute of Standards and Technology, US
National Aerospace Laboratory, Japan
National Aerospace Laboratory, Netherlands

SPARES (10 copies)

Total number of copies: 70

DEFENCE SCIENCE AND TECHNOLOGY ORGANISATION
DOCUMENT CONTROL DATA

1. PRIVACY MARKING/CAVEAT (OF DOCUMENT)

2. TITLE

Structural Shape Optimisation by Iterative Finite Element Solution

3. SECURITY CLASSIFICATION (FOR UNCLASSIFIED REPORTS THAT ARE LIMITED RELEASE USE (L) NEXT TO DOCUMENT CLASSIFICATION)

Document	(U)
Title	(U)
Abstract	(U)

4. AUTHOR(S)

R. Kaye and M. Heller

5. CORPORATE AUTHOR

Aeronautical and Maritime Research Laboratory
PO Box 4331
Melbourne Vic 3001

6a. DSTO NUMBER	6b. AR NUMBER	6c. TYPE OF REPORT	7. DOCUMENT DATE
DSTO-RR-0105	AR-010-247	Research Report	June 1997

8. FILE NUMBER	9. TASK NUMBER	10. TASK SPONSOR	11. NO. OF PAGES	12. NO. OF REFERENCES
M1/9/272	Air 95/228	AIR OIC ASI-LSA	42	18

13. DOWNGRADING/DELIMITING INSTRUCTIONS

None

14. RELEASE AUTHORITY

Chief, Airframes and Engines Division

15. SECONDARY RELEASE STATEMENT OF THIS DOCUMENT

Approved for public release

OVERSEAS ENQUIRIES OUTSIDE STATED LIMITATIONS SHOULD BE REFERRED THROUGH DOCUMENT EXCHANGE CENTRE, DIS NETWORK OFFICE, DEPT OF DEFENCE, CAMPBELL PARK OFFICES, CANBERRA ACT 2600

16. DELIBERATE ANNOUNCEMENT

No Limitations

17. CASUAL ANNOUNCEMENT Yes

18. DEFTEST DESCRIPTORS

stress concentration, finite element analysis

19. ABSTRACT

This report presents the development and automated numerical implementation of an iterative gradientless optimisation method for the analysis of problems relating to life extension of aircraft components. The method has been implemented to interface with the finite element code PAFEC, which does not normally have an optimisation capability. The key feature of the approach is to achieve constant boundary stresses, in regions of interest, by moving nodes on the stress concentrator boundary by an amount dependent on the sign and magnitude of the local hoop stress obtained from a previous iteration of a standard finite element analysis. The results of example problems are presented which include the optimisation of hole shapes in flat plates and the optimisation of the design of bonded reinforcements with a focus on minimising adhesive stress while maintaining the effectiveness of the reinforcement. In all cases significant stress reductions were achieved by way of the local shape changes. The method presented is considered a simple robust complementary method to the use of commercially available gradient based finite element optimisation software. It is also considered suitable for use with typical standard commercial finite element packages other than PAFEC.